2009

PduL is an evolutionary distinct phosphotransacylase involved in B12-dependent 1,2-propanediol degradation by Salmonella enterica serovar Typhimurium LT2 and is associated with the propanediol utilization microcompartments

Yu Liu
Iowa State University

PduL is an evolutionary distinct phosphotransacylase involved in B_{12}-dependent 1,2-propanediol degradation by *Salmonella enterica* serovar Typhimurium LT2 and is associated with the propanediol utilization microcompartments

by

Yu Liu

A thesis submitted to the graduate faculty

in partial fulfillment of the requirements for the degree of

MASTER OF SCIENCE

Major: Immunobiology

Program of Study Committee:
Thomas Bobik, Major Professor
Louisa Tabatabai
Qijing Zhang
Kenneth J. Koehler

Iowa State University

Ames, Iowa

2009

TABLE OF CONTENTS

LIST OF FIGURES

LIST OF TABLES

LIST OF ABBREVIATIONS

1,2-PD	1,2 propanediol
3-AT	3-amino-1,2,4-triazole
3-PGA	3-phosphoglycerate
AdeCbl	adenosylcobalamin
AEBSF	4-(2-Aminoethyl)benzenesulfonylfluoride HCl
Amp	ampicillin
ATP	adenosine triphosphate
B-PER II	bacterial protein extraction reagent II
CA	carbonic anhydrase
CCM	CO_2-concentrating mechanism
CH_3Cbl	methylcobalamin
CNCbl	cyanocobalamin
Cob	cobalamin
CoA	coenzyme A
DDH	diol dehydratase
Dmb	dimethylbenzimidazole
E. Coli	*Escherichia coli*
EDTA	ethylenediaminetetraacetic acid
HCl	hydrogen chloride
His_8	8 C-terminal histidine residues
HPLC	high pressure liquid chromatography
HPLC-ESI-MS	HPLC electrospray ionization mass spectrometry

IgG	immunoglobulin G
AP	alkaline phosphatase
KanR	kanamycin resistance
IPTG	isopropyl-β-D-thiogalactopyranoside
LB	luria-bertani/Lennox
MALDI-TOF MS	matrix assisted laser desorption ionization-time-of-flight mass spectrometry
Mcp	microcompartment
NCE	no-carbon-E
PAGE	polyacrylamide gel electrophoresis
PCR	polymerase chain reaction
pI	isoelectric point
pdu	propanediol utilization
PSI-BLAST	protein specific iterative basic local alighment search tool
Pta	phosphotransacetylase
PTAC	phosphotransacylase
PVDF	polyvinylidene fluoride
RuBisco	ribulose bis-phosphate carboxylase monooxygenase
RuBP	ribulose bisphosphate
SDS	sodium dodecyl sulfate
S. enterica	*Salmonella enterica*
s.n.	supernatant
Tn	transposon

ABSTRACT

Salmonella enterica degrades 1,2-propanediol (1,2-PD) in a coenzyme B_{12}-dependent manner. Prior enzymatic assays of crude cell extracts indicated that a phosphotransacylase (PTAC) was needed for this process, but the enzyme involved was not identified. Here we show that the *pduL* gene encodes an evolutionarily distinct PTAC used for 1,2-PD degradation. Growth tests showed that *pduL* mutants were unable to ferment 1,2-PD and were also impaired for aerobic growth on this compound. Enzyme assays showed that cell extracts from a *pduL* mutant lacked measurable PTAC activity in a background that also carried a *pta* mutation (the *pta* gene was previously shown to encode a PTAC enzyme). Ectopic expression of *pduL* corrected the growth defects of *pta* mutant. PduL fused to 8 C-terminal histidine residues (PduL-his_8) was purified and its kinetic constants determined: V_{max} = 51.7±7.6 μmol min^{-1} mg^{-1}; and K_m for propionyl-PO_4^{2-} and acetyl-PO_4^{2-} = 0.61 and 0.97 mM, respectively. Sequence analyses showed that PduL is unrelated in amino acid sequence to known PTAC enzymes and that PduL homologues are distributed among at least 49 bacterial species, but are absent from the Archaea and Eukarya. Immunoblots showed that PduL was a component of propanediol utilization microcompartment. PduL enzyme assay and two-hybrid analysis indicated PduL was associated with several candidate partner proteins including PduJK, PduB', PduM, PduN and PduW expressed from *pdu* operon.

INTRODUCTION

Cobalamin B_{12}

Vitamin B_{12} which is also known as cyanocobalamin (CNCbl) is a precursor of two coenzymes, adenosylcobalamin (AdoCbl) and methylcobalamin (CH_3Cbl). These coenzymes are required cofactors for a variety of enzymes found in bacteria and higher animals. CH_3Cbl-dependent enzymes catalyze a variety of methyl transfer reactions and AdoCbl-dependent enzymes mediate difficult rearrangements and reductions via free radical mechanisms. Two human enzymes that require B_{12} are known and these enzymes are vital for good health. Among the Bacteria and Archaea, about 15 different B_{12}-dependent enzymes have been reported and several have important biotechnology applications.

Structure of AdoCbl

AdoCbl has a molecular weight of 1580, and at least 25 enzymes are uniquely involved in its synthesis. The AdoCbl molecule has three parts: a central ring, an adenosyl moiety, and a nucleotide loop. The central ring is structurally and biosynthetically related to those of heme and chlorophyll. AdoCbl also has a 5' deoxyadenosyl moiety serving as its upper (Coβ) axial ligand; the 5' carbon of this ribose group is joined by a covalent bond to the cobalt within the corrin ring. Cobalt's lower (Coα) axial ligand is the N-7 of dimethylbenzimidazole (Dmb). The Dmb moiety is attached covalently to the corrin ring as part of a nucleotide loop. The nucleotide, 3' phosphoribosyl-Dmb, is linked through its phosphate to an aminopropanol moiety that is attached to a propionyl group extending from the D porphyrin of the corrin ring (41).

B_{12} –Dependent Reactions in Enteric Bacteria

The enzymes listed below are found in one or more species of enteric bacteria.

PROPANEDIOL DEHYDRATASE

This enzyme, which converts 1,2-propanediol to propionaldehyde, is found in virtually all enteric bacteria tested except *Escherichia coli* (42, 37). Some bacteria ferment propanediol by oxidizing a portion of the propionaldehyde to provide carbon and energy while reducing the rest to provide an electron sink for balancing redox reactions (43). In *Salmonella* species this process provides energy but no carbon source. Propanediol is encountered frequently by bacteria, because it is produced during anaerobic catabolism of the common methylpentoses, rhamnose and fucose (44).

ETHANOLAMINE AMMONIA LYASE

This enzyme converts ethanolamine to acetaldehyde and ammonia (45, 46). Under some conditions, the produced acetaldehyde can serve as a carbon and energy source via acetyl-CoA. Ethanolamine is frequently encountered in nature as part of common lipids, phosphatidyl ethanolamine and phosphatidyl choline.

GLYCEROL DEHYDRATASE

This enzyme converts glycerol to β-hydroxypropionaldehyde, which can be reduced to 1, 3 propanediol (1, 47). This reaction balances the reducing equivalents generated by glycerol dehydrogenase. Glycerol dehydratase is common in enterics but is absent from both *Salmonella spp.* and *E. coli* (42).

METHIONINE SYNTHETASE

This enzyme transfers a methyl group from methyl-tetrahydrofolate to homocysteine as the final step in synthesis of methionine and is probably the best-known B_{12}-dependent reaction (96, 97). The lack of this reaction underlies many aspects of human B_{12}-deficiency disorders (95).

B_{12} Synthesis in *Salmonella enterica* and *Cob* Operon

Most of the B_{12} synthetic genes are located in a single, 20-gene operon that maps near minute 44 of the *S. enterica* chromosome (48,49,50). As more mutations were classified, several (*cobA, cobB, cobC, cobD, and cysG*) were found to map outside of the main operon. These unlinked biosynthetic genes appear to contribute to assimilation of exogenous B_{12} precursors or to play secondary roles in some process other than cobalamin de novo synthesis. Thus the main *cob* operon contains only genes needed for de novo B_{12} synthesis; the unlinked genes may have additional functions that are important even when B_{12} is not being synthesized de novo. The exact functions of some of these unlinked genes are not yet clear.

1,2-Propanediol

A number of bacterial genera including *Salmonella, Klebsiella, Shigella, Yersinia*, *Listeria*, *Lactobacillus* and *Lactococcus* grow on 1,2-PD in a coenzyme B_{12}-dependent fashion. 1,2-PD is a major product of the fermentation of rhamnose and fucose which are common sugars in plant cell walls, bacterial exopolysaccharides and the glycoconjugates of intestinal epithelial cells. Accordingly, the ability to degrade 1,2-PD is thought to provide a selective advantage in anaerobic environments such as the large intestines of higher animals, sediments and the depths of soils. Recent studies with *S. enterica* have shown that 1,2-PD

degradation is one of the most complex metabolic processes known (6, 14, 15, 18, 19, 31). The degradation of this small molecule requires catabolic enzymes, a system for recycling inactive cobalamins to coenzyme $B_{12,}$ and an unusual polyhedral body that is composed of metabolic enzymes encased within a multi-protein shell. If one includes cobalamin biosynthetic genes which are contiguous and coregulated with propanediol utilization (pdu) genes, *Salmonella enterica* retains 40-50 genes primarily for the transformation of propanediol (6).

Pathway for 1,2-PD Degradation

A pathway for 1,2-PD degradation by *S. enterica* has been proposed based on enzymatic studies of crude cell extracts and genetic analyses (25, 37). In the first step of the pathway, 1,2-PD in converted to propionaldehyde via coenzyme B_{12}-dependent diol dehydratase (1). Propionaldehyde is then converted to propionyl-CoA by the CoA-dependent propionaldehyde dehydrogenase (1,25,37). Propionyl-CoA can be converted to 1-propanol by 1-propanol dehydrogenase or to propionic acid by a reaction series thought to involve coenzyme A (CoA)-dependent propionaldehyde dehydrogenase, phosphotransacylase (PTAC), and propionate kinase (25, 37). This pathway generates one ATP, an electron sink, and a 3-carbon intermediate (propionyl-CoA), which feeds into central metabolism via the methylcitrate pathway (16).

Metabolism of 1,2-PD under Anaerobic and Aerobic Conditions

When grown anaerobically on L-rhamnose, *S. enterica* excreted 1,2-propanediol as a fermentation product. Upon exhaustion of the methyl pentose, 1,2-propanediol was recaptured and further metabolized, provided the culture was kept under

anaerobic conditions. n-Propanol and propionate were found in the medium as end products of this process at concentrations one-half that of 1,2-PD. A series of enzymes used here were CoA-dependent propionaldehyde dehydrogenase, propionaldehyde dehydrogenase, alcohol dehydrogenase, phosphate acetyltransferase and acetate kinase (25). The intermediate aldehyde can be oxidized to form propionyl-CoA or alternatively can be reduced to form propanol. By forming and excreting propanol, cells can balance internal redox reactions. Under anaerobic conditions, propionyl-CoA can be converted by a phosphotransacylase to propionyl-phosphate, and then by a reversible acetyl-/propionyl-kinase to propionate, producing one molecule of ATP (51). According to this scheme, anaerobic metabolism of propanediol could provide an electron sink (propionaldehyde) and a source of ATP but no source of carbon since propanol and propionate are excreted (41). Under aerobic conditions, *S. enterica* can use propionyl-CoA as both a carbon and an energy source，propionyl-CoA can be converted to propionyl-phosphate and then propionate producing ATP or enter central metabolism by way of the methylcitrate pathway.

***pdu* Locus**

The genes specifically required for 1,2-PD utilization (*pdu*) by *S. enterica* form a single contiguous cluster, the *pdu* locus. DNA sequence analyses indicate that this locus includes 23 genes (6, 7, 10). Based on experimental and/or bioinformatic analyses, six *pdu* genes are thought to encode enzymes needed for the 1,2-PD degradative pathway (6); two are involved in transport and regulation (5, 10); two are probably involved in diol dehydratase reactivation (6); two are used for the

conversion of vitamin B_{12} to coenzyme B_{12} (18, 31); four are of unknown function; and seven share similarity to genes involved in the formation of carboxysomes, a polyhedral body found in certain cyanobacteria and chemoautotrophs (6, 10). Although the methylcitrate pathway is required for growth of *S. enterica* on 1,2-PD a sole carbon source, the genes for this pathway map outside the *pdu* locus (16).

Regulation of *pdu* Operon

The genes for degradation of 1,2-PD are coregulated with genes for cobalamin (Vitamin B_{12}) biosynthesis. Both the *pdu* and *cob* operons are induced by 1,2-PD by means of PocR, a positive regulatory protein of the AraC-family (10). This coregulation of a synthetic and a degradative pathway reflects the fact that Vitamin B_{12} is a required cofactor for the first enzyme in propanediol breakdown. The *pdu* and *cob* operons form a single regulon. Propanediol induces the regulon either aerobically or anaerobically during growth on poor carbon sources (5). The *cob/pdu* regulon is induced by propanediol under two sets of growth conditions, i.e. during aerobic respiration of a poor carbon source and during anaerobic growth. Under aerobic conditions, the Crp/cyclic AMP system is needed for all induction of the *pocR, cob*, and *pdu* genes. Anaerobically, the Crp/cyclic AMP and ArcA/ArcB systems, a two component redox control system that acts under anaerobic conditions to repress synthesis of proteins involved in aerobic respiration act additively to support induction of the same three transcription units. The Crp/cyclic AMP complex is the primary global regulator of *pocR* under aerobic conditions, while maximal anaerobic induction requires the additive effects of both the Crp/cyclic AMP complex and the ArcA/ArcB system (52). The control of the regulon depends on five promoters, all located in the

central region between the *cob* and *pdu* operons; four of these promoters are activated by the PocR protein (53).

The current model for control of this system includes the following features (see Figure 1): The *cob* and *pdu* operons are transcribed divergently from promoters indicated at the far right and left in the figure. These promoters are activated whenever both the PocR protein and propanediol are present. Global control of the two operons is exerted by varying the level of PocR protein. The *pocR* gene is transcribed by three promoters controlled both by global regulatory proteins and by autoinduction. The shortest transcript (from Ppoc) appears to be regulated only by Crp/cAMP. The P2 transcript clearly is autoregulated by PocR and, in addition, requires the ArcA protein, which signals a reduced cell interior (53). Control of the P1 promoter is less certain but may involve either the Fnr protein (responding to a reduced cell interior) or the Crp protein (responding to a shortage of carbon and energy) in addition to the PocR activator. The involvement of these proteins in control of P1 is based heavily on the presence of appropriate binding sites upstream of that promoter. JR Roth et al (41) propose that the regulon has three states. In the off condition (during aerobic growth on glucose), all promoters are at their lowest level; PocR protein is produced by the basal expression levels of promoters P1, P2, and Ppoc. Cells enter a standby state when they grow under any set of global conditions appropriate for induction, but without propanediol. These conditions include aerobic growth on a poor carbon source and/or growth without oxygen. These conditions stimulate expression of both the PduF transporter and the PocR regulatory protein, but the *cob* and *pdu* operons remain uninduced. The stand by expression of PocR

can occur from the Ppoc and/or the P1 promoter without inducer. The two proteins induced in the standby state (PduF and PocR) are those needed to sense propanediol. If propanediol appears, the P1 and P2 promoters are induced, increasing the level of PocR protein and placing the system in the on state. The resulting high level of PocR/propanediol complex induces expression of the *cob* and *pdu* promoter.

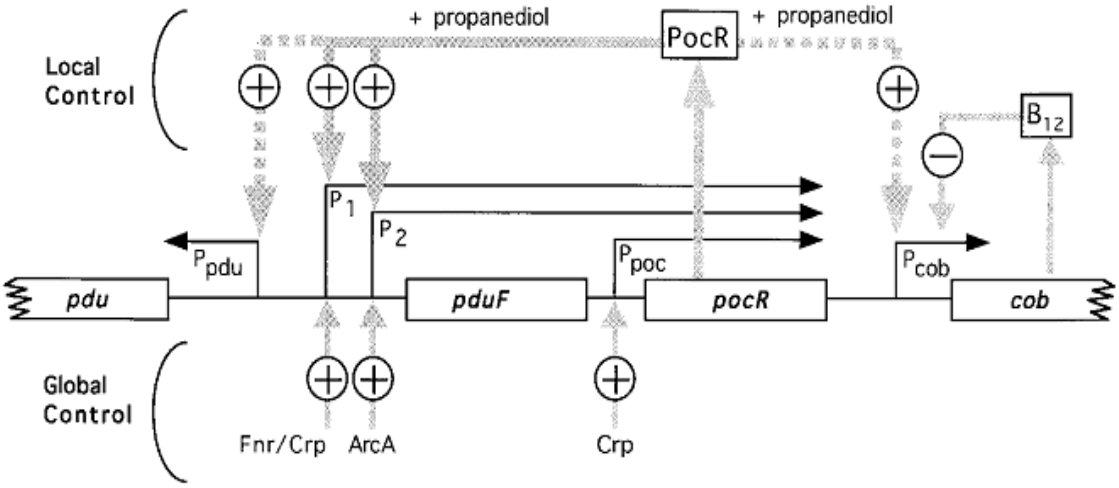

Fig. 1. Regulation of the *cob/pdu* regulon of *Salmonella enterica* (41). The genetic map describes the region between *pdu* and *cob* operons whose transcripts start at the far sides of the figure. Boxes enclose structural genes. Black arrows designate transcripts (53). Gray arrows indicate regulatory influence; dashed gray arrows indicate the proposal that a higher level of PocR protein may be required to activate these promoters.

Bacterial Microcompartments

Recent studies indicate that proteinaceous microcompartments are widely used by bacteria to optimize particular metabolic processes (4, 54, 55). Physiological studies and genomic analyses tentatively indicate seven functionally distinct microcompartment distributed among over 40 genera of bacteria. As yet, such compartments have not been found in the Archaea or Eukarya. The microcompartments that have been studied consist of a solid protein shell that encapsulates sequential metabolic enzymes (14, 56, 57). Studies indicate that the general role of the protein shell is to sequester toxic or volatile metabolic intermediates; however, it must also allow enzyme substrates, products and cofactors to pass (4, 58). Current models for microcompartment function propose that a selectively permeable shell and a highly defined architecture mediates the necessary molecular routing (56, 58).

Carboxysome

Carboxysomes were the first bacterial microcompartments identified. They were observed more than 50 years ago as polyhedral bodies in the cytoplasm of cyanobacteria (59). They play a key role in enhancing autotrophic carbon fixation via the Calvin cycle, and they are widely distributed among chemoautotrophs and cyanobacteria (55, 58, 60, 61). Carboxysomes are very large and sophisticated multi-protein complexes (Fig. 2a). They are about 80–150 nm in cross section and are bounded by a 3–4 nm thick protein shell. Their mass is about 300 MDa and they are composed of several thousand polypeptides of 10–15 different types (62, 63). The lumen or interior of the carboxysome contains the sequential metabolic enzymes

carbonic anhydrase (CA) and ribulose bis-phosphate carboxylase monooxygenase (RuBisCO) (57, 64). CA converts HCO_3^- to CO_2 within the carboxysome, then RuBisCO converts CO_2 and ribulose bisphosphate (RuBP) to two molecules of 3-phosphoglycerate (3-PGA). The shell of the carboxysome is proposed to retain CO_2 in the immediate vicinity of RuBisCO by acting as a diffusion barrier (65, 66). In vivo, the carboxysome works in conjunction with C1 transport systems as part of a bacterial CO_2-concentrating mechanism (CCM) that is used to increase the level of CO_2 in the local vicinity of RuBisCO thereby enhancing carbon fixation and autotrophic growth (58).

Composition of Carboxysome

Investigations conducted thus far indicate that carboxysomes (and other microcompartments) are made completely of protein subunits (14, 67, 68). There are no confirmed reports of RNA, DNA, or lipids associated with carboxysomes or other microcompartments. No lipid bilayer or monolayer is visible by electron microscopy under conditions where such structures would be readily apparent. However, the possibility of associated lipids is an open question. It has been reported that two carboxysome proteins (CsoS2A and CsoS2B) are glycosylated (69), but other occurrences of carbohydrates are unknown.

α- and β-Carboxysomes

A variety of studies indicate two main classes of carboxysomes, α and β, which varies slightly in composition. Each class is thought to have co-evolved with a different phylogenetic group of RuBisCO (70, 71). Theα-carboxysome is associated with form 1A RuBisCO which is found in chemoautotrophs and α-cyanobacteria while

theβ-carboxysome is associated with form 1B RuBisCO which is found in the β-cyanobacteria (71). Overall, α- and β-carboxysomes are thought to have similar architectural and mechanistic principles. The gene names differ betweenα- and β-carboxysomes. However, many of their protein components are conserved with the exceptions that the CsoS2 and CsoS3 proteins are specific to type α while the CcmM, CcmN and CcaA proteins are characteristic of typeβ(70, 72).

Carboxysome Genomics

The number and organization of carboxysome genes varies somewhat among different organisms reflecting the compositional variation between typesα and βand also suggesting some minor variations within type. The best-studied α-carboxysome is that of *H. neapolitanus*. This organism has the following carboxysome gene cluster: *cbbL-cbbS-csoS2-csoS3-csos4A-csos4B-csoS1C-csoS1A-csoS1B* (72). In general, α-carboxysome gene clusters are conserved with the exception that one copy of CsoS1 is sometimes found at the start of the cluster adjacent to the ccbL gene.

β-carboxysome has been studied in several cyanobacteria. In *Synechocystis* PCC 6803, theβ-carboxysome genes are arranged as follows: *ccmN-ccmM-ccmL-ccmK- ccmK//ccmK-ccmK//ccaA//rbcL-rbcX-rbcS//ccmO* (72). The arrangement in *Synechococcus elongatus* PCC 7942 is *ccmK-ccmK//ccmK-ccmL-ccmM-ccmN-ccmO-rbcL-rbcS// ccaA//rbcX*. As is the case for theα-carboxysome there is the possibility of additional β-carboxysome genes yet to be identified.

Carboxysomes are Icosahedral

For many years, there was uncertainty about the overall shape of carboxysomes. Electron microscopy suggested they were either icosahedra or pentagonal dodecahedra (73, 74). However, recent electron cryotomography of carboxysomes from *Synechococcus* strain WH8102 (β-type) and *H. neapolitanus* (α-type) indicate an icosahedral structure (75, 76). The shells of these carboxysomes appear 3–4 nm thick and their sizes range from 114–137 nm for *Synechococcus* and from 88–108 nm for *H. neapolitanus*. The molecular mass range is estimated to be 115–355 MDa for *H. neapolitanus* carboxysomes (76). About 250 RuBisCO molecules could be visualized per carboxysome arranged in 3–4 concentric layers, but well-defined interactions between the RuBisCO subunits and the shell were not evident (76, 77).

Molecular Conduits for Small Molecules Span the Carboxysome Shell

Current models for carboxysome function require that its shell is permeable to RuBP, HCO_3^- and 3-phosphoglycerate, but restricts the diffusion of CO_2 (58). Crystallography of its protein subunits suggests that the carboxysome shell is essentially solid except for small pores and gaps (56, 63, 78). The CcmK1, CcmK2 and CcmK4 hexamers have central pores that range in diameter from 4 or 6 Å taking vander Waals radii into account, and the boundaries where these hexamers join to form sheets have gaps 4–6 Å wide (56, 79). The central pores have a large net positive electrostatic potential and the boundary gaps also have conserved positively charged amino acid residues. These findings suggest that the pores and gaps could act as molecular conduits that preferentially allow negatively charged molecules such as RuBP, HCO_3^- and 3-phosphoglycerate to pass while restricting the movement of uncharged molecules such as CO_2 and possibly O_2. Similar openings are found in the

corresponding shell protein (CsoS1A) from *H. neapolitanus* further supporting the importance of these features (78). In the carboxysomes of *Synechocystis* PCC6803 and *H. neapolitanus*, the pentameric proteins thought to occupy the vertices of the shell also have narrow pores (63). However, the small number of pentamers compared to hexamers in the shell suggests that transport across these pores might not be significant.

Propanediol Utilization Microcompartment

For many years, carboxysomes were the only known bacterial microcompartment. Then, in 1994, genetic studies indicated that a BMC-domain protein was involved in B_{12}-dependent 1, 2-propanediol degradation by *S.enterica* (10). A few years later, electron microscopy showed that *S. enterica* conditionally formed microcompartments during B_{12}-dependent growth on 1,2-propanediol and further studies established that microcompartments function in this process (6, 15, 36, 54). The Pdu microcompartments are extremely large multi-protein complexes that are generally similar to carboxysomes in size and appearance (Fig. 2b). They are 100–150 nm in cross section with a 3-4 nm protein shell. Their shape is roughly polyhedral, but they are more irregular than carboxysomes. Their mass is about 600 MDa and they are composed of about 18,000 individual polypeptides of about 14–18 different types (84). Like carboxysomes, the Pdu microcompartments are thought to be composed completely from protein subunits (14). The proposed function of the Pdu microcompartments is to sequester an intermediate of 1,2-propanediol degradation (propionaldehyde) in order to prevent toxicity and diffusive loss (15, 86). Thus, there may be functional analogy between the Pdu microcompartments and

carboxysomes in that both are used to confine metabolic intermediates that are not well-retained by lipid bilayers.

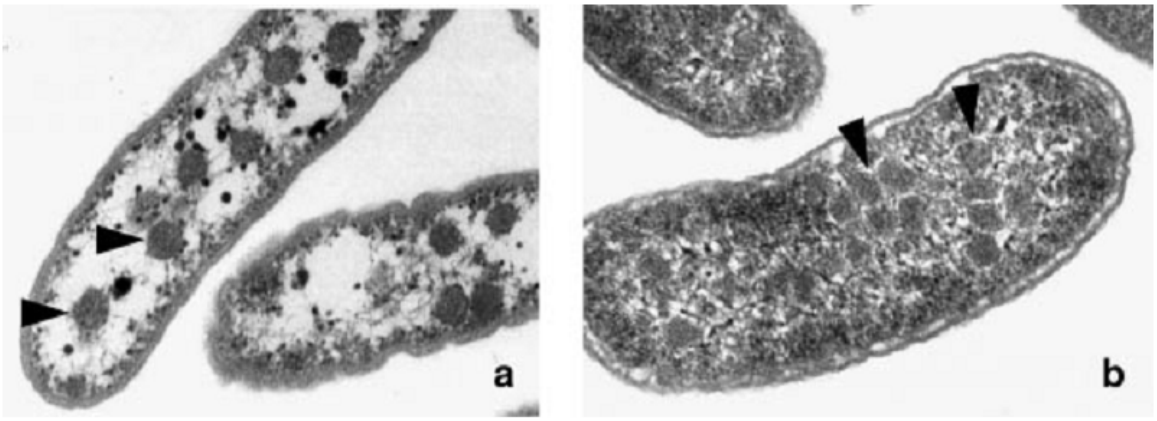

Fig. 2. Electron micrograph of bacterial microcompartments (4): a: The carboxysomes of *H. neapolitanus;* b: The organelles formed during growth of *Salmonella enterica* on 1,2-propanediol. Triangles point to the microcompartments.

Model for the Pdu Microcompartment

The current model for the Pdu microcompartment proposes that the first two steps of 1,2-propanediol degradation are confined to the lumen of a microcompartment so that propionaldehyde can be sequestered (14) (Fig. 3). In the model, 1,2-propanediol traverses the microcompartment shell and enters the lumen where it is converted to propionaldehyde by B_{12}-dependent diol dehydratase. Propionaldehyde dehydrogenase then catalyzes the conversion of propionaldehyde + HS-CoA + NAD^+ →propionyl-CoA + NADH + H^+ (14, 19). Propionyl-CoA continues through the 1,2-propanediol degradative pathway to propionate and 1-propanol, or enters the

methylcitrate pathway where it is converted to pyruvate and succinate (25, 37, 86). These processes allow *S. enterica* to grow efficiently on 1,2-propanediol as a sole carbon and energy source while at the same time sequestering propionaldehyde. Confinement of propionaldehyde allows its rate of production and consumption to be matched, mitigating toxicity and DNA damage and reducing diffusive loss to the environment since propionaldehyde is poorly retained by lipid bilayers (86). In the model, two additional enzymes are placed in the lumen of the Pdu microcompartment: diol dehydratase reactivase (PduGH) and adenosyltransferase (PduO). These enzymes support the activity of diol dehydratase by ensuring an adequate supply of coenzyme B_{12} (18, 87).

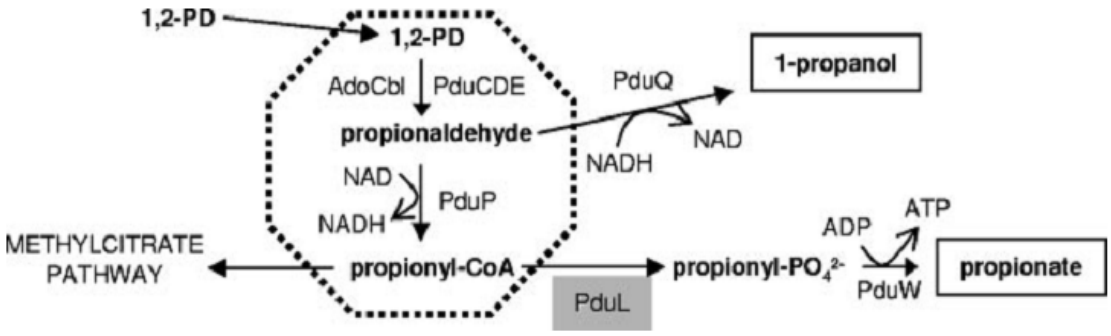

Fig. 3. Model for 1,2-propanediol degradation by *S. enterica*. Coenzyme B_{12} (AdoCbl), coenzyme B_{12}-dependent diol dehydratase (PduCDE), propionaldehyde dehydrogenase (PduP), phosphotransacylase (PduL), propionate kinase (PduW), and 1-propanol dehydrogenase (PduQ) are depicted. The first two steps of 1,2-PD degradation (conversion of 1,2-PD to propionyl-CoA) are proposed to occur within Pdu microcompartments. The dashed line indicates the shell of the microcompartments, which is composed of up to seven different polypeptides. ATP is generated during the conversion of propionyl-PO_4^{2-} to propionate. Given a suitable terminal electron acceptor such as O_2, propionyl-CoA is degraded via the methylcitrate pathway, where biosynthetic precursors and additional energy are produced. Two additional enzymes associated with the polyhedral bodies (but not shown in the figure) are a putative diol dehydratase reactivase (PduGH) and an ATP:cob(I)alamin adenosyltransferase (PduO) involved in B_{12} recycling.

Proteomics of the Pdu Microcompartments

The protein content of the Pdu microcompartment supports the functional model described above. The Pdu microcompartments were purified intact (Fig.4) (14). They consist of 14 different major polypeptides (PduABB'CDEGHJKOPTU) (14). Four of the components of the Pdu microcompartment are enzymes: (i) B_{12}-dependent diol dehydratase (PduCDE), (ii) diol dehydratase reactivase (PduGH), (iii) adenosyltransferase (PduO), and (iv) propionaldehyde dehydrogenase (PduP). This complement of enzymes supports the idea that the first two steps of 1,2-propanediol degradation occur within the microcompartments, and this is confirmed by enzyme assays that show purified Pdu microcompartments have high levels of diol dehydratase and propionaldehyde dehydrogenase activity (14, 19). The remaining enzymes of the 1,2-propanediol degradative pathway (propionate kinase, and 1-propanol dehydrogenase) are not detected in purified Pdu microcompartments suggesting that these enzymes localize to the cytoplasm of the cell (14). The protein content of the Pdu microcompartments also supports the idea of a shell consisting of seven different BMC-domain proteins (PduABBJKTU), a somewhat more complex arrangement than the shell of the *H. neapolitanus* carboxysome, which is composed of three different BMC domain proteins (14). Thus, protein content underpins many aspects of the current model for the Pdu microcompartment. A caveat of these studies is that low-abundance components of the Pdu microcompartment may have escaped detection, as is likely the case for the protein that is suggested to form the vertice of the carboxysome shell (63).

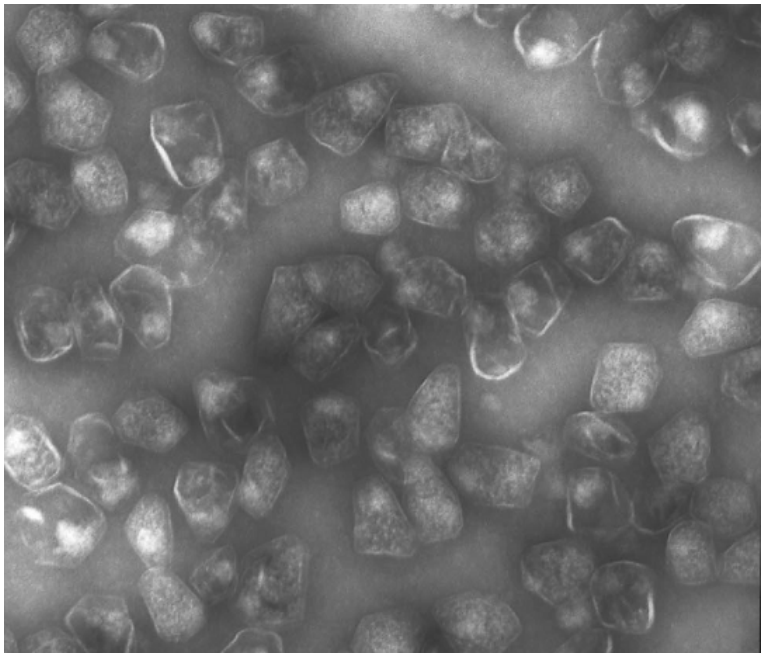

Fig. 4. Electron micrographs of Pdu microcompartments from S. enterica, Magnification, 53,000 (14).

The Pathway of 1,2-Propanediol Degradation

The pathway of 1,2-propanediol degradation presented in figure 3 is well-established by genetic and biochemical studies. The overall pathway was first outlined by biochemical studies of whole cells and crude cell extracts (25, 37). B_{12}-dependent diol dehydratase, propionaldehyde dehydrogenase, phosphotransacylase, and propionate kinase have been studied in vitro, and their substrates, products and cofactor requirements have been defined (7, 19, 26). Their encoding genes have been identified (6, 7, 19, 26). Knockout mutations have established their role in 1,2-propanediol degradation in vivo (6, 7, 17, 19, 26). The 1-propanol dehydrogenase has not yet been studied, but its encoding gene has been

identified and 1-propanol has been established as a product of 1,2-propanediol degradation (6, 86). The role of diol dehydratase reactivase (PduGH) and adenosyltransferase in 1,2-propanediol degradation has been established by genetic tests (18, 84). Adenosyltransferase has been characterized biochemically (18, 80, 84) and the properties of reactivase are inferred from studies on a closely related enzyme from *Klebsiella* (87, 88, 89).

The Genetics of 1,2-Propanediol Degradation

The genetics of 1,2-propanediol degradation further supports model 1 in figure 3 and suggests some additional components may be involved in microcompartment formation. In *S. enterica*, the genes involved in 1,2-propanediol degradation are organized as a contiguous, twenty-three-gene cluster on centisome 44 of the chromosome with the following structure: *pocR, pduF, pduABCDEGHJKLMNOPQSTUVWX* (6). This locus is one of the largest clusters of functionally related genes found in *S. enterica*. It encodes a transcriptional regulator (PocR), a 1,2-propanediol facilitator (PduF), three enzymes for B_{12} metabolism (PduGH, PduO, and PduS), one enzyme used for the de novo synthesis of B_{12} (PduX), five catabolic enzymes that mediate 1,2-propanediol degradation as described above (PduCDE, PduL, PduP, PduQ, PduW), seven BMC-domain proteins (PduA, PduB, PduB', PduJ, PduK, PduT and PduU), the *pduA* and *pduB* genes encode a close and distant relative of carboxysome shell proteins, a protein with homology to the pentamer proposed to form the carboxysome vertices (PduN) and two polypeptides of unknown function (PduM and PduV) (5, 6, 10, 18, 26, 31, 90). *S. enterica* strains with deletions of the *pduM* gene form abnormal microcompartments

suggesting that the PduM protein may play a structural role (84). Pfam analyses indicated that the PduV protein is related to the AAA-family of ATPases, but its role in 1,2-propanediol degradation is unknown.

Assembly of Microcompartments

Genetic deletion of each lumen enzyme individually does not preclude the formation of the shell (14, 19, 80). Hence, no single lumen enzyme of the Pdu microcompartments is required as a scaffold for shell formation. A particularly interesting aspect of organelle assembly which is currently poorly understood is the manner in which proteins are targeted to the lumen. Several proteins that reside in the lumen of polyhedral organelles have N- or C-terminal extensions by comparison to homologous proteins found in the cell cytoplasm. For example, two of the three subunits of B_{12}-dependent DDH which are found in the lumen of the Pdu microcompartments have short N-terminal extensions compared to their cytoplasmic homologs. Removal of these extensions dramatically increases the solubility of DDH but does not affect its catalytic activity appreciably (81). A targeting apparatus that directs proteins to the lumen of microcompartments is possible.

Mitigation of Aldehyde Toxicity and Diffusive Loss

The first evidence that microcompartments might have a role in mitigating aldehyde toxicity was based on comparative genetics (86). Sequence analyses showed that both 1,2-propanediol and ethanolamine degradation involve BMC domain proteins (10, 86). A common feature of the 1,2-propanediol and ethanolamine degradative pathways is that both proceed through aldehyde intermediates (propionaldehyde and acetaldehyde, respectively); hence, it was proposed that

microcompartments might be formed to sequester aldehydes which were known cytotoxins (86). Later studies showed that mutants unable to form the Pdu microcompartments accumulated large amounts of propionaldehyde and underwent a temporary period of growth arrest due to propionaldehyde toxicity (15, 86). In addition, propionaldehyde was found to be a mutagen and mutation frequencies were increased in microcompartment mutants during growth on 1,2-propanediol (86). The aldehyde toxicity model is further supported by the findings that *polA* (DNA repair polymerase) and *gsh* (glutathione biosynthesis) mutants were unable to grow on ethanolamine (91, 92). However, other studies have indicated that the main role of the ethanolamine microcompartment might be to prevent the loss of a volatile metabolic intermediate, acetaldehyde (28). In the case of propionaldehyde (boiling point=48℃), loss due to volatility appears less important than for acetaldehyde (boiling point=20℃) (86).

Homologues of Carboxysome Proteins

The CcmK protein has been reported to be a shell protein of the carboxysome (82). Two genes of the *eut* operon (*eutM* and *eutK*) and one of the *pdu* operon (*pduA*) encode homologues of the CcmK protein of *Synechococcus* sp. (10). PduA and PduJ proteins are closely related to carboxysome shell proteins Csos1A, Csos1B, Csos1C, CcmK, and CcmO (50–60% identity). The PduK and PduT proteins are 25–30% identical to CsoS1.The PduN proteinis 46% identical to carboxysome protein CcmL from *Synechococcus elongatus* PCC 6301 and distantly related to the putative carboxysome proteins encoded by *orfA* and *orfB* of *H. neapolitanus*. In addition, position-specific iterated–basic local alignment search tool (PSI-BLAST) analyses

show that the PduB and PduU proteins are distantly related to the carboxysome shell proteins CcmK and CsoS1 (4). Another *eut* gene (*eutN*) encodes a homologue of a different carboxysome structural protein (CcmL of *Synechococcus* sp.). In addition, the PduB and EutL proteins share significant homology to each other but not to other proteins in the database, suggesting a role common to the two pathways.

Structure of the Pdu Microcompartments

The structure of the Pdu microcompartments is a key to resolving its functional principles. At this time, its structure can be tentatively modeled based on its protein content and analogy with the carboxysome. Carboxysomes are proposed to be icosahedra with triangular faces made from hexamers of BMC-domain proteins and vertices formed from pentamers with homology to the CcmL and CsoS4 proteins (63). According to the crystal structure of two carboxysome shell proteins CcmK2 and CcmK4 monomers are wedge-shaped and fit tightly together, forming a solid hexamer having a central pore. The pores of the CcmK2 and CcmK4 hexamers are 7 and 4 Å, respectively, and have a large net positive electrostatic potential. There are 4- to 6-Å-wide gaps between the hexamers that also feature conserved charged amino acids. Both the hexamer pores and the gaps between hexamers could potentially serve as conduits for metabolites, and it was proposed that these pores might selectively allow passage of negatively charged molecules such as the substrates and products of RuBisCO while restricting uncharged molecules such as CO_2 and O_2 (56). Purified Pdu microcompartments contain two major BMC-domain proteins (PduA and PduJ) that are closely related in sequence to the hexamers proposed to form the faces of the carboxysome (14). The *pdu* operon also encodes a

homolog of the pentamer proposed to form the vertices of the carboxysome (PduN) (63). Thus, analogy suggests that the shell of the Pdu microcompartments may have faces made from PduA and PduJ hexamers and vertices made from PduN pentamers. However, electron microscopy shows that the Pdu microcompartments are more irregular in shape than carboxysomes suggesting they vary somewhat from a regular icosahedron and may include distinctive structural elements (14, 15, 94). In addition, the Pdu microcompartment includes seven BMC domain proteins whereas carboxysomes generally have 3–5. The crystal structure of one of these shell proteins, PduU, has been determined and shown to differ substantially from the homologous carboxysome shell proteins (93). This suggests that the shell of the Pdu microcompartments may be more sophisticated than that of the carboxysome which would not be surprising considering its complement of enzymes and their cofactor requirements.

Research Overview

It was recently shown that *S. enterica* forms microcompartments during growth on 1,2-PD (6, 15, 36). The first two steps of 1,2-PD degradation are thought to occur in the lumen of the Pdu microcompartments, and the remaining steps are thought to occur in the cytoplasm of the cell (14). Previous studies suggested that they function to sequester propionaldehyde (an intermediate of 1,2-PD degradation) in order to minimize toxicity and/or prevent carbon loss (9, 14, 15, 28). Interestingly, recent

genomic analyses tentatively indicated that there are seven functionally distinct microcompartments distributed among over 40 genera of bacteria (4). Thus, microcompartments may be a general mechanism of metabolic organization in the bacteria.

Prior enzymatic analysis of crude cell extracts indicated that a PTAC is used for 1,2-PD degradation (25, 37). However, the enzyme involved was not identified. The first part of this study investigates the genetic and biochemical evidence of the involvement of PduL protein in B_{12}-dependent 1,2-propanediol degradation. Growth tests were done to study the impairment of 1,2-propanediol degradation for *pduL* mutation aerobically and anaerobically. Complementation studies were performed to further examine the functions of PduL in vivo. Enzyme assays and HPLC-ESI-MS were also used to determine biochemical characteristics of PduL protein. Finally kinetic studies with purified PduL-His_8 were performed to better understand the catalytic mechanism of enzyme PduL.

The second part of this study investigated the relationship between PduL protein and Pdu microcompartments. The PduL protein was cloned, overexpressed, purified, and then used to generate polyclonal antiserum for use in immunoblotting studies. Once it was established that PduL was part of Pdu microcompartments a series of enzyme assays and two-hybrid analysis were conducted to screen the candidate partner proteins from microcompartments which might interact with PduL protein in some way.

MATERIALS AND METHODS

Chemicals and Reagents.

Antibiotics, vitamin B_{12} and acetyl-PO_4^{2-} were from Sigma Chemical Company (St. Louis, MO). Propionyl-PO_4^{2-} was synthesized as described (27). Isopropyl-β-D-thiogalactopyranoside (IPTG) was from Diagnostic Chemicals Limited (Charlotteville PEI, Canada). Restriction enzymes and T4 DNA ligase were from New England Biolabs (Beverly, MA). goat anti-mouse IgG-AP conjugate, PVDF membrane, AP Conjugate Substrate Kit, Coomassie Brilliant Blue R-250, EDTA, ethidium bromide, 2-mercaptoethanol, and SDS were from Bio-Rad (Hercules, CA). lysozyme was from Sigma-Aldrich (St. Louis, MO). Anti-PduL antiserum was from Hybridoma Facility Iowa State University (Ames, IA). BacterioMatch II Two-Hybrid System Library Construction Kit was from Stratagene (Cedar Creek, TX). Other chemicals were from Fisher Scientific (Pittsburgh, PA).

Bacterial Strains, Media, and Growth Conditions.

The bacterial strains used in this study are listed in Table 1. The rich medium used was Luria-Bertani/Lennox (LB) medium (Difco, Detroit, MI) (23). The minimal media used was no-carbon-E (NCE) medium containing supplements indicated in the text and figure legends (3, 38). MacConkey/1,2-PD indicator medium contained MacConkey agar base (Difco), 1% 1,2-PD and 200 ng ml^{-1} of vitamin B_{12}. the minimal media used for BacterioMatch II two-hybrid assays was $M9^+$ medium added with 0.4% glucose, His dropout amino acid, adenine hydrogen chloride (HCl) and Thiamine HCl together with 3-amino-1,2,4-triazole (3-AT) and antibiotics tetracycline and chloramphenicol.

Table 1. Bacterial strains used in this study

Species	Strain	Genotype
[a]*S. enterica* serovar Typhimurium LT2		
	BE47	*thr-480::Tn10dCam*
	BE188	Δ*pduL670*
	BE281	*pta-406*::Tn*10*
	BE284	Δ*pduL670* /pLAC22-*pduL* (AmpR)
	BE285	Δ*pduL670* /pLAC22-*no insert* (AmpR)
	BE286	pLAC22-*pduL* (AmpR)
	BE287	pLAC22-no insert (AmpR)
	BE291	*ΔpduL670 pta-209*::Tn*10*
	BE527	*pta-209*::Tn*10*
	BE529	*pta-209*::Tn*10* /pLAC22-no insert (AmpR)
	BE530	*pta-209*::Tn*10* /pLAC22-*pduL* (AmpR)
	BE548	*pta-209*::Tn*10* /pBE522-no insert (KanR)
	BE549	*pta-209*::Tn*10* /pBE522-*pta* (KanR)
	BE712	*ΔpduUT pta-209*::Tn*10*
	BE717	*ΔpduABB' pta-209*::Tn*10*
	BE721	*ΔpduJK pta-209*::Tn*10*
	BE729	*ΔpduP pta-209*::Tn*10*
	BE730	*ΔpduW pta-209*::Tn*10*
E.coli		
	BL21(DE3)RIL	(*E. coli* B) F^-*ompT hsdS* ($r_B^-m_B^-$) *dcm*$^+$ Tet^r *gal* (DE3) *endA* Hte (*argU ileY leuW* Cam^r)
	BE303	BL21(DE3)RIL /pta925-*pdu*L

[a]Formerly *S. typhimurium* LT2

General Molecular Methods.

Agarose gel electrophoresis was performed as described previously (30). Plasmid DNA was purified by the alkaline lysis procedure (30) or by using Qiagen products (Qiagen, Chatsworth, CA) according to the manufacturer's instructions. Following restriction digestion or PCR amplification, DNA was purified using

Promega Wizard PCR Preps (Madison, WI) or Qiagen gel extraction kits. Restriction digests were carried out using standard protocols (30). For ligation of DNA fragments, T4 DNA ligase was used according to the manufacturer's directions. Electroporation was carried out as previously described (6).

Protein Methods.

Polyacrylamide gel electrophoresis (PAGE) was performed using Bio-Rad Redigels and Bio-Rad Mini-Protean II electrophoresis cells according to the manufacture's instructions. Following gel electrophoresis, Coomassie Brilliant Blue R-250 was used to stain proteins. The protein concentration of solutions was determined using Bio-Rad Protein Assay Reagent (Bio-Rad).

P22 Transduction.

Transductional crosses were performed as described using P22 HT105/1 *int*-210 (12), a mutant phage that has high transducing ability (32). Transductants were tested for phage contamination and sensitivity by streaking on green plates against P22 H5.

Construction of Plasmids for Production of PduL and PduL-his$_8$.

PCR was used to amplify the *pduL* coding sequence from template pMGS2 (15). The primers used for amplification were 5'-GCCGCCAGATCTATGGATAAAGAGCTTCTGCAATCA-3' and 5'-GCCGCCAAGCTTATTATCGCGGGCCTACCAGCCG-3'. These PCR primers introduced *Bgl*II and *Hin*dIII restriction sites that were used for cloning into vector pLAC22 (39). Following ligation, clones were introduced into *E coli* DH5α by electroporation and transformants were selected by plating on LB agar supplemented

with 100 μg ml^{-1} ampicillin (Amp) (18). Pure cultures were prepared from selected transformants. The presence of insert DNA was verified by restriction analysis or PCR, and the DNA sequence of selected *pduL* clones was determined. Clones having the expected DNA sequence were used for further study.

A similar procedure was used to clone PduL fused to eight C-terminal histidine residues (PduL-his_8) with the following differences. The primers used for PCR amplification were 5'-GCCGCCAGATCTATGGATAAAGAGCTTCTGCAATCA-3' and 5'-GCCGCCAAGCTTATTAATGATGATGATGATGATGATGATGTCGCGGGCCTAC CAGCCG-3. The PCR product was ligated to T7 expression vector pTA925 (18). Transformation was done by electroporation and LB plates supplemented with 25 μg ml^{-1} kanamycin (Kan) were used to select for transformants.

Growth of the PduL-his_8 Production Strain.

A T7 expression plasmid (pTA925) was used for production of PduL-his_8. The host used for protein expression was *E. coli* BL21DE3 RIL (Stratagene). This strain expresses T7 RNA polymerase as well as rare tRNAs for arginine, isoleucine and leucine. Expression and control strains (BE554 and BE119) were grown in 400 ml LB broth containing 25 μg/ml Kan and 10 μg/ml chloramphenicol. Cultures were incubated at 15 °C with shaking at 275 rpm in a 1 liter baffled Erlenmeyer flask. Cells were grown to an optical density of 0.6-0.8 at 600 nm and protein expression was induced by the addition of 1 mM IPTG. Cells were incubated for an additional 16 hours, and harvested by centrifugation at 8,000 x *g* for 10 minutes and at 4 °C using a Beckman JA-10 rotor and Avanti J-25 centrifuge.

Purification of PduL-his_8.

The PduL-his_8 production strain (BE554) was grown as described above. One gram of cells (wet weight) was suspended in 3 ml of buffer containing 50 mM Tris-HCl, pH 7.2, 200 mM $(NH_4)_2SO_4$ and 0.4 mM AEBSF. Cells were broken using a French pressure cell at 20,000 psi, and the resulting cell extract was centrifuged at 20,000 x *g* using a Beckman JA-17 rotor. The supernatant fraction was filtered through a 0.45 µm syringe filter. A chromatography column containing 1 ml of Ni-NTA resin (Qiagen) was equilibrated with 5 ml of buffer A: 50 mM Tri-HCl, pH 7.7, 25 mM KCl, 300 mM NaCl, 200 mM $(NH_4)_2SO_4$ 10 mM imidazole and 5 mM 2-mercaptoethanol. Filtered cell extract (2.5 ml, about 50 mg protein) was applied to the column. The column was washed with 15 ml of buffer A supplemented with 10% glycerol and 80 mM imidazole. The column was eluted with 10 ml of buffer A (in two of 5 ml steps) supplemented with 10% glycerol and 400 mM imidazole.

Preparation of Cell Extracts of *S. enterica*.

Cells were grown under conditions that induce the *pdu* operon (5). Cell paste was suspended in 25 mM Tris-HCl, pH 7.2 containing 0.4 mM protease inhibitor 4-(2-Aminoethyl)benzenesulfonylfluoride·HCl (AEBSF) (3 ml of buffer per gram cells wet weight). Cells were broken using a French pressure cell (Thermo Electron Corp., Waltham, MA) at 20,000 psi.

PTAC Assays.

PTAC assays measured the conversion of acyl-PO_4^{2-} + HS-CoA to acyl-CoA, and were performed as described (21). Standard assays contained 50 mM Tris-HCl, pH 7.2, 20 mM KCl, 0.2 mM HS-CoA, and 1 mM acyl-PO_4^{2-} in a total volume of 1 ml. For kinetic studies, the concentrations of certain assay components were varied as

indicated in the text. Activity was determined by following absorbance at 232 nm over time and by using E_{232} = 5.5 mM^{-1} cm^{-1} for calculations.

Construction of a Nonpolar *pduL* Deletion.

Bases 22 to 612 of the *pduL* coding sequence were deleted via a PCR-based method (24). The deletion was designed to leave all predicted translational start and stop signals of *pdu* genes intact. The following primers were used for PCR amplification of the flanking regions of the *pduL* gene: primer 1, 5'-GCTCTAGAGCCGAAATCAGCCTAATCGATGGCG-3'; primer 2, 5'-CGTTCATCGCGGGCCTACCAGCCGATCCATTACGCTTCACCTCGC-3'; primer 3, 5'-CGGCTGGTAGGCCCGCGATGAACG-3'; and primer 4, 5'-CGAGCTCGCCAGATGCATGATTTACTC-3'. Primers 1 and 2 were used to amplify a 498 base-pair region upstream of the *pduL* gene, and primers 3 and 4 were used to amplify 527 bases downstream of *pduL* gene. The upstream and downstream amplification products were purified then fused by a PCR reaction that included 1 ng/µl of each product and primers 1 and 4. The fused product was digested with *Xba*I and *Sac*I (these sites were designed into primers 1 and 4, respectively), and ligated to suicide vector pCVD442 that had been similarly digested. The ligation mixture was used to transform *E. coli* S17.1 by electroporation and transformants were selected on LB medium supplemented with Amp (100 µg/ml). Six transformants were screened by restriction analysis and all released an insert of the expected size (1058 bp). One of these transformants was used to introduce the *pduL* deletion into the *S. enterica* chromosome using the procedure of Miller and Mekelanos (24) with the following modification. For the conjugation step, strain

BE47 was used as the recipient and exconjugants were selected by plating on LB agar supplemented with Amp (100 μg/ml) and chloramphenicol (20 μg/ml). Deletion of the *pduL* coding sequence was verified by PCR using chromosomal DNA as a template. Lastly, the *thr-480* dCAM insertion used for selection of exconjugants was "crossed-off" by P22 transduction using a phage lysate prepared with the wild-type strain and by selecting for prototrophy on NCE glucose minimal medium.

Aerobic Growth Curves.

Growth media are described in the figure legends. For strains carrying pLAC22, media were also supplemented with 100 μg/ml Amp and 0.2 mM IPTG. To prepare the inoculum, LB cultures (2 ml) were incubated overnight at 37 °C, and then cells were collected by centrifugation and resuspended in growth curve medium. Media were inoculated to a density of 0.15 AU and growth was followed by measuring optical density at 600 nm using a BioTek Synergy microplate reader as follows: 48-well flat bottom plates (Falcon); 0.5 ml of growth medium per well, 37 °C; and shaking set a level 4. A relatively low volume of growth medium (0.5 ml) in a 48-well microplate was necessary for adequate aeration and controls showed that growth under these conditions was similar to growth in shake flasks (data not shown).

Anaerobic Growth Curves.

A procedure similar to that for aerobic growth curves was used to measure the fermentation of 1,2-PD, but with the following differences. Cultures were inoculated to an initial density of 0.1 AU. Microplates were sealed with polyolefin membranes (Fisher Scientific) inside an anaerobic growth chamber (Coy Laboratory Products, Grass Lake, MI). To monitor whether anaerobic conditions were maintained within

the microplate, NCE glycerol minimal medium was added to several wells and inoculated with wild-type *S. enterica. S. enterica* cannot ferment glycerol; therefore, growth on glycerol would indicate the presence of oxygen. For the experiments described in this study, no growth was observed in wells containing glycerol minimal medium indicating that the headspace contained minimal amounts of oxygen (data not shown).

DNA Sequencing and Analysis.

DNA sequencing was carried out at the Iowa State University (ISU) DNA Facility using Applied Biosystems Inc. automated sequencing equipment. The template for DNA sequencing was plasmid DNA purified using Qiagen 100 tips or Qiagen mini-prep kits. BLAST software was used for sequence similarity searching (2).

High-Pressure Liquid Chromatography (HPLC).

A Microsorb C_{18} column (150 x 4.6 mm) was used with a Varian ProStar system that included a model 230 solvent delivery module, a model 430 autosampler and a model 325 UV-Vis detector (Varian, Palo Alto, CA). Buffer A and B contained 10 mM NH_4 formate pH 4.6 and 10% or 90% methanol, respectively. The flow rate was 1 ml min^{-1} and the buffer composition was varied as follows: (minute: %B), 0:0, 5:0, 17:100, 22:100, 23:0, 28:0.

HPLC Electrospray Ionization Mass Spectrometry (HPLC-ESI-MS).

An Agilent ion trap model 1100 mass spectrometer (Agilent, Palo Alto, CA) was operated in the positive mode. The ion source parameters were optimized for the formation of [M+H]+ ions with source temperature of 310 °C, capillary voltage of 3.2

kV, and cone voltage of 25 V. Nitrogen was used as the nebulizing gas and as the drying gas at flow rates of 15 and 400 L h^{-1}, respectively.

PTAC Assays for Shell Encoding Gene Mutants.

400ml cells were incubated in NCE minimal medium supplemented with 0.5% succinate and 0.6% 1,2-PD until OD600 reached 1-1.2. Cells were harvested by centrifugation at 8,000 x *g* using a Beckman JA-17 rotor and resuspended in breaking buffer (50mM Tris-HCl pH7.2, 200mM 1M $(NH_4)_2SO4$, 0.5mM petabloc). Cells were broken using a French pressure cell at 20,000 lb/in^2, and the resulting cell extract was centrifuged at 25,000 x *g* for 25 min at 4°C using a Beckman JA-17 rotor to separate soluble fraction and the pellet. Cell crude extracts, s.n. fractions and the pellets were measured immediately.

PTAC assays measured the conversion of propionyl-PO_4^{2-} + HS-CoA to propionyl-CoA, and were performed as described (21). Standard assays contained 50 mM Tris-HCl, pH 7.2, 20 mM KCl, 0.2 mM HS-CoA, and 1 mM propionyl -PO_4^{2-} in a total volume of 1 ml. For kinetic studies, the concentrations of certain assay components were varied as indicated in the text. Activity was determined by following absorbance at 232 nm over time and by using E_{232} = 5.5 mM^{-1} cm^{-1} for calculations.

Pdu Microcompartments Purification.

Cells (400ml) were incubated in NCE minimal medium supplemented with 0.5% succinate and 0.6% 1,2-PD until OD600 reached 1-1.2. Cells were harvested by centrifugation at 6,000 x *g* using a Beckman JA-17 rotor and washed with 40ml buffer A (50 mM Tris-HCl pH 8.0, 500mM KCl, 25 mM NaCl, 12.5 mM MgCl2 and 1.5% 1,2-PD). The pelleted cells were resuspended in same buffer such that the final

volume is 10 ml per gram of cells wet weigh. 1.0 mM ABESF, 2.5 mg/ml lysozyme and 2 mg DNAase in 1.5 volumes of B-PER II were added to the resuspended cells and incubated at room temperature for 30 min using Innova 2000 at 50-70 rpm. Unlysed cells and cell debris were removed by centrifugation at 12,000 x *g* for 5 min twice, and the resulting supernatant was then subjected to centrifugation at 20,000 x *g* for 20 min. The pellet was resuspended in a solution containing 4 ml Buffer A, 6 ml BPERII, 0.4 mM AEBSF, and 0.5 mg/ml lysozyme and incubated at room temperature for another 10 min using Innova 2000 at 50-70 rpm, then was pelleted by centrifugation at 20,000 x *g* for 20 min. The pellet was resuspended in cold buffer B (50 mM Tris-HCl pH 8.0, 50mM KCl, 5 mM $MgCl_2$ and 1% 1,2-PD) and then clarified by centrifugation for 5 min using an Eppendorf 5417R microcentrifuge. The supernatant containing the purified Pdu microcompartments was carefully removed and stored at 4°C prior to analysis.

Antibody Preparation.

His_8-PduL protein obtained from Ni^{2+} affinity chromatography (see above) was resolved on a 12% polyacrylamide gel. The portion of the gel containing the PduL protein was excised and used as a source of antigen. Polyclonal antibodies were prepared in mouse by the Hybridoma Facility of Iowa State University.

Western Blot.

Purified Pdu microcompartments (10 µg) were subjected to sodium dodecyl sulfate polyacrylamide gel electrophoresis (SDS-PAGE) using a 12% ready gel (Bio-Rad). Electro-blotting was performed in 25 mM Tris, pH 8.3, 192 mM glycine, 0.1% SDS, 20% Methanol using Mini Trans-Blot Cell (Bio-Rad)., run at 400 mA

constant for 40 min at 4°C using a PowerPac Basic power supply (Bio-Rad). PVDF Membranes (Bio-Rad) were probed as described previously (83) using anti-PduL polyclonal antibodies diluted 1:500 in blocking buffer as the primary antibody and goat anti-mouse immunoglobulin G-alkaline phosphatase conjugate (Bio-Rad) diluted 1:3,000 in blocking buffer as the secondary antibody. Color developing reagents were used as specified in the manufacturer's directions (Bio-Rad).

Two-Hybrid Screening.

Bacteria two-hybrid screening was performed according to the manufacturer's protocols (Stratagene). The *pBT-pduL* construct and each of genes from *pdu* operon fused to pTRG were co-transformed into the BacterioMatch II Electrocompetent Reporter Cells. The co-transformants were plated on His drop-out selective screening medium containing 5 mM 3-amino-1,2,4- triazole (3-AT) for 24 hours at 37℃ and then for 2-3 days at 30℃ to induce the expression of reporter proteins fused with the activation domain. pBT-LGF2 cotransformed with pTRG-Gal11^{p} was used as positive control, and pBT cotransformed with pTRG-*pdu* genes was used as negative control. Positive colonies were confirmed on His drop-out dual selective screening plates containing 5 mM 3-AT and streptomycin.

RESULTS

The *pta* Gene is Nonessential for 1,2-PD Degradation.

Prior biochemical studies indicated that PTAC was needed for 1,2-PD degradation by *S. enterica* (25, 37). In the proposed biochemical pathway, this enzyme catalyzed the conversion of propionyl-CoA to propionyl-phosphate (transfer of a 3-carbon acyl-group) (Fig.3). An enzyme with homology to known PTAC enzymes is not encoded by the *pdu* locus (6). However, *S. enterica* produces a phosphotransacetylase (Pta) encoded by the *pta* gene which maps outside the *pdu* operon at centisome 50 (20). Pta is used for growth on acetate and inositol and plays a key role in the interconversion of acetyl-CoA and acetyl-PO_4^{2-} (transfer of a 2-carbon acyl-group) (20). In vitro, Pta not only mediates the interconversion of acetyl-CoA and acetyl-phosphate, it also catalyzes the interconversion propionyl-CoA and propionyl-PO_4^{2-} (20, 35). This raised the question of whether *pta* plays a role in 1,2-PD degradation. Two independent *pta* mutants (BE281 and BE527) were examined for growth on 1,2-PD. Aerobically, both grew slightly faster than wild-type *S. enterica*. The doubling times for the wild-type were typically 7.5-8.5 h and those for the *pta* mutants were 6-7 h. Both *pta* mutants were reconstructed via P22 transduction to assure that they were isogenic with the wild-type and both still exhibited a small increase in growth rate on 1,2-PD (not shown). These results confirmed prior studies which showed that *pta* is nonessential for aerobic growth of *S. enterica* on 1,2-PD minimal medium (26).

Similarly, *pta* was unnecessary for the fermentation of 1,2-PD. Strains with *pta* mutations and wild-type *S. enterica* both had doubling times of 5-6 h during 1,2-PD

fermentation. Phenotypic test showed that the *pta* mutants used in the above studies were impaired for grow on acetate or inositol minimal medium and lacked detectable *pta* activity in cell extracts as is expected for *pta* mutants (20). In addition, the growth defects on acetate and inositol were corrected by a *pta* minimal clone and the chromosomal location of both *pta* insertions was verified by PCR (data not shown). Hence, we conclude that the *pta* gene is nonessential for B_{12}-dependent 1,2-PD degradation under either aerobic or anaerobic growth conditions.

Strains with *pduL* Mutations Produce Less Propionic Acid on MacConkey / 1,2-Propanediol Indicator Medium.

The finding that the *pta* gene was unnecessary for 1,2-PD degradation suggested that *S. enterica* expresses an additional PTAC that is sufficient to mediate this process. As part of ongoing studies of 1,2-PD degradation by *S. enterica*, we constructed a series of precise *pdu* deletion mutations using PCR-based methods (11, 24). Tests with MacConkey/1,2-PD medium (17) indicated that three independent *pduL* deletion mutants each produced less propionic acid from 1,2-PD than did wild-type *S. enterica*. The enzymes that convert 1,2-PD to propionic acid were proposed to include coenzyme B_{12}-dependent diol dehydratase, propionaldehyde dehydrogenase, propionate kinase and PTAC (Fig. 1) (25, 37). Of these, only the gene for the PTAC was unidentified (7, 19, 26). Hence, these results tentatively suggested that the *pduL* gene encodes a PTAC enzyme.

Enzyme Assays Indicate that *pduL* Encodes a PTAC Enzyme.

Wild-type *S. enterica*, as well as *pduL* and *pta* null mutants were grown under conditions that induce the *pdu* operon (5). Cell extracts were prepared and PTAC

activity was measured using an assay that follows the conversion of acyl-phosphate + HS-CoA to acyl-CoA and inorganic phosphate (the reverse reaction with respect to 1,2-PD degradation). Both propionyl-PO_4^{2-} and acetyl-PO_4^{2-} were used as substrates. Cell extract from the wild-type strain had 8.9 μmol min^{-1} mg^{-1} PTAC activity with propionyl-PO_4^{2-} (Table 2). Extracts from *pta* or *pduL* mutants had partial activity (6.0 and 2.6 μmol min^{-1} mg^{-1}, respectively) (Table 2). PTAC activity was undetectable in cell extracts from the double mutant (*pta pduL*). The simplest interpretation of these results is that *pduL* and *pta* each encode PTAC enzymes which was previously shown for *pta* (20). Furthermore, the *pta pduL* double mutant lacked detectable PTAC activity demonstrating that the activity in Pta^- $PduL^+$ cell extracts required PduL.

Enzyme assays also showed that the PTAC in Pta^- $PduL^+$ cell extracts was 15-fold more active with propionyl-PO_4^{2-} compared to acetyl-PO_4^{2-} (6 μmol min^{-1} mg^{-1} compared to 0.4 μmol min^{-1} mg^{-1}) (Table 2). This is consistent with a role for PduL in 1,2-PD degradation. On the other hand, the PTAC activity in Pta^+ $PduL^-$ cell extracts was 1.6-fold more active with acetyl-PO_4^{2-} consistent with the role of Pta in acetyl-group metabolism (20).

For the above enzyme assays, controls showed that detectable PTAC activity required acyl-phosphate and HS-CoA, and in all cases PTAC activity was linear with enzyme concentration (data not shown).

TABLE 2. Phosphotransacylase activity in cell extracts from selected strains of S. enterica[a]

Strain (relevant genotype)	PTAC activity (μmol min^{-1} mg^{-1})[b]		
	Propionyl-PO_4^{2-}	Acetyl-PO_4^{2-}	Propionyl-PO_4^{2-} preference[c]
Wild type (PduL$^+$ Pta$^+$)	8.9	3.5	2.5
BE188 (PduL$^-$ Pta$^+$)	2.6	3.2	0.8
BE527 (PduL$^+$ Pta$^-$)	6.0	0.4	15.0
BE291 (PduL$^-$ Pta$^-$)	ND	ND	

[a]Cells were grown on NCE succinate minimal medium supplemented with 1,2-PD to ensure induction of the pdu operon.

[b]PTAC assay mixtures contained 0.2 mM HS-CoA and 1 mM propionyl-PO_4^{2-} or acetyl-PO_4^{2-} and assay buffer. Activity was determined by monitoring the absorbance of reaction mixtures at 232 nm. ND, not detected (the lower detection limit of the assay is estimated to be 0.03 μmol min^{-1} mg^{-1}.

[c]Propionyl-PO_4^{2-} preference (activity with propionyl-PO_4^{2-})/(activity with acetyl- PO_4^{2-}).

pduL Mutants are Impaired for Aerobic Growth on 1,2-PD.

Compared to wild-type *S. enterica*, a *pduL* mutant (BE188) was impaired for aerobic growth on 1,2-PD (Fig. 5A). The doubling time for *S. enterica* was 7.9±0.5 h and that of a *pduL* mutant was 12.6±0.6 h. Further impairment of growth was not seen in the *pduL pta* double mutant even though this mutant lacked measurable PTAC activity (data not shown). These findings are consistent with the idea that PduL is a PTAC involved in 1,2-PD degradation. Aerobically, growth on 1,2-PD is expected to proceed in the absence of PTAC since propionyl-CoA (which is formed prior to the PTAC reaction) can be metabolized via the methylcitrate pathway (Fig. 3) (16). The

observed growth impairment of the *pduL* mutant was likely due to reduced ATP synthesis resulting from a block in the oxidative branch of the 1,2-PD degradative pathway although other explanations cannot be ruled out.

***pduL* Mutants are Unable to Obtain Energy from 1,2-PD under Fermentative Conditions.**

In the absence of an exogenous electron acceptor, the methylcitrate pathway is inoperative, and *S. enterica* is unable to grow on 1,2-PD as a sole carbon source (29). Under these conditions, *S. enterica* converts 1,2-PD to 1-propanol and propionate (Fig. 3). This stimulates growth on minimal medium supplemented with a small amount of yeast extract by providing a source of ATP (29). The production of ATP via the conversion of 1,2-PD to propionate is expected to require PTAC (Fig 3). Therefore, we tested the effect of a *pduL* mutation on this process. The doubling times of wild-type *S. enterica* in the presence and absence of 1,2-PD under fermentative conditions were 5.5±0.35 h and 10.7±0.29 h, respectively (Fig. 5B); the fermentation of 1,2-PD stimulated the growth rate about 2-fold which is consistent with previous studies (29). The doubling times of the *pduL* mutant (BE188) under fermentative conditions in the presence and absence of 1,2-PD were 13.1±1.0 and 13.3±0.95 h, respectively. This indicated that energy production via 1,2-PD fermentation was completely eliminated by the *pduL* mutation. This is consistent with a role for PduL in 1,2-PD degradation.

The *pduL* mutant used in the above studies contained a wild-type *pta* gene indicating that Pta did not substitute for PduL under the conditions used to measure the 1,2-PD fermentation. Furthermore, a *pta* null mutation (alone or in combination

with a *pduL* null mutation) did not affect the fermentation of 1,2-PD (data not shown). These results indicate that the Pta enzyme is insufficient to support the fermentation of 1,2-PD and that PduL is required.

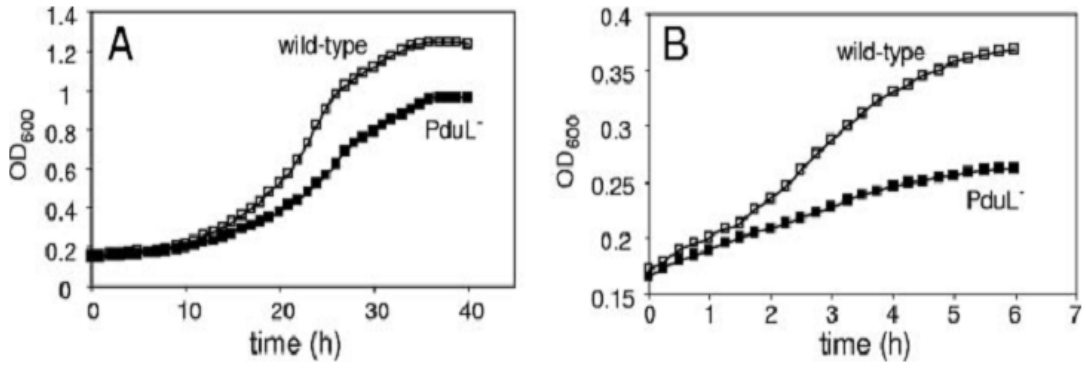

Fig. 5. Growth of a pduL null mutant on 1,2-PD. (A) Aerobic growth of wild-type *S. enterica* and a *pduL* mutant (BE188) on 1,2-PD minimal medium. (B) Fermentation of 1,2-PD. BE188 carries a precise deletion of the *pduL* gene made by a PCR-based method. The observed growth defects of BE188 were corrected by a *pduL* minimal clone. Each growth curve was performed three times in quadruplicate. Representative curves are shown. Log-phase doubling times with standard deviations are given in the text. The aerobic growth medium was NCE supplemented with 52 mM 1,2-PD, 200 ng ml^{-1} vitamin B_{12}, and 0.3 mM valine, isoleucine, leucine, and threonine. The fermentation medium was NCE supplemented with 52 mM 1,2-PD, 200 ng ml^{-1} vitamin B_{12}, and 0.2% yeast extract. The inoculation and incubation procedures are described in Materials and Methods. OD_{600}, optical density at 600 nm.

The Observed Phenotypes of a *pduL* Mutant are Complemented by a *pduL* Minimal Clone.

Growth tests showed that the aerobic and anaerobic growth phenotypes described above for a *pduL* mutant (BE188) were fully corrected by expression of a

pduL minimal clone using a tightly regulated expression vector, pLAC22. Under aerobic conditions, the doubling times BE287 (wild-type S*. enterica*/pLAC22-no insert) and BE286 (wild-type *S. enterica*/pLAC22-*pduL*) were 5.4 ±0.12 h compared to 6.0±0.32 h, respectively. The doubling times for strains for BE285 (*pduL*/pLAC22-no insert) and BE284 (*pduL*/pLAC22-*pduL*) were 8.2 ±0.71 and 5.5 ±0.25 h, respectively. Under anaerobic conditions, the doubling times *S. enterica*/pLAC22-no insert, *S. enterica*/pLAC22-*pduL*, *pduL*/pLAC22-no insert and *pduL*/pLAC22-*pduL* were 5.0±0.22, 5.2±0.37, 11.1±0.19, and 5.3±0.40 respectively. Thus, under aerobic and anaerobic conditions, a *pduL* minimal clone complemented the growth defect to the *pduL* mutation. On the other hand, vector without insert did not correct the observed growth defects of the *pduL* mutant. These results show that observed phenotypes of *pduL* mutant (BE188) resulted from the deletion of the *pduL* gene, but not from polarity or a mutation acquired during strain construction.

PduL Substitutes for Pta in Vivo During Acetate Utilization.

Growth tests were performed to determine whether PduL could substitute for Pta in vivo. Prior studies showed that *pta* mutants grow very slowly on minimal medium with >30 mM acetate (20). Here we show that ectopic expression of PduL corrects this defect (Fig. 6). The doubling times of the Pta^+ strain and the *pta* mutant on acetate minimal medium were 4.4±0.41 and 28.6±1.4 h, respectively. The doubling time of a *pta* mutant producing PduL from expression vector pLAC22 was 3.7±0.1 h which was slightly faster than the control (4.4±0.41). Hence, ectopic expression of *pduL* fully corrected the growth defect of the *pta* mutant on acetate minimal medium.

Since Pta is a well-studied PTAC enzyme, this finding indicates that PduL also has PTAC activity.

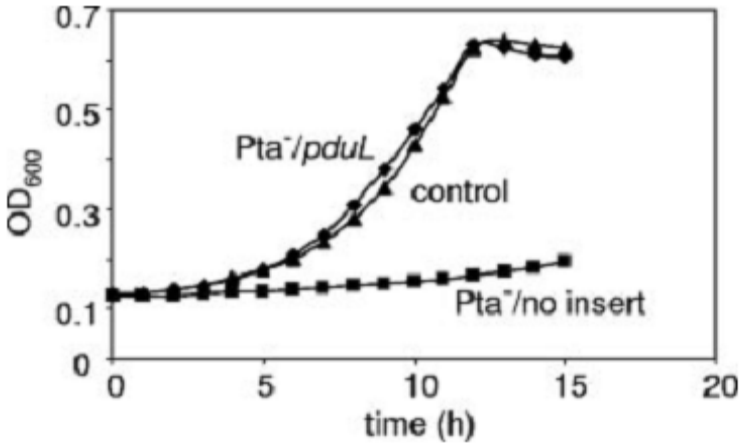

Fig. 6. Ectopic expression of a *pduL* minimal clone corrects the growth defect of a *pta* mutant on acetate minimal medium. Data for *S. enterica* harboring expression vector pLAC22 without an insert (control), a *pta* mutant carrying pLAC22 without an insert (Pta⁻ /no insert), and a *pta* mutant harboring a *pduL* minimal clone in pLAC22 (Pta⁻/*pduL*) are shown. The relevant strains are BE287, BE529, and BE530 (Table 1). Controls showed that pLAC22 with or without the *pduL* insert did not observably affect the growth of the wild-type strain on acetate minimal medium (data not shown). In addition, the growth defect of the *pta* mutant was fully corrected by a *pta* minimal clone, showing that the effects of this mutation were not due to polarity (data not shown). The growth medium was NCE supplemented with 0.2% Na acetate and 0.2 mM IPTG. Each growth study was performed twice in quadruplicate. Representative curves are shown. Log-phase doubling times with standard deviations are given in the text. OD_{600}, optical density at 600 nm.

Propionyl-CoA is a Product of the PduL Reaction.

The finding that HS-CoA was required for PduL activity (see above) indicated that an acyl-CoA was formed in assay mixtures. Moreover, the PTAC assay used to

measure PduL activity followed absorbance at 232 nm which monitors the formation of thioester bonds (13). To confirm that an acyl-CoA was formed in PduL enzyme assays, HPLC and HPLC-mass spectrometry were performed. Assays containing cell extract from BE527 (Pta^- $PduL^+$) or BE291 (Pta^- $PduL^-$), HS-CoA, propionyl-PO_4^{2-} and standard components; therefore, propionyl-CoA was the expected acyl-CoA product. Reverse-phase HPLC with UV detection at 260 nm was used to identify CoA compounds present in reaction mixtures. A single major compound with a retention time of 10.9 min was detected when Pta^- $PduL^+$ cell extracts were used. This compound co-eluted with authentic propionyl-CoA following co-injection and produced a mass spectrum characteristic of propionyl-CoA via HPLC-ESI-MS (Fig. 7). The major peaks for authentic propionyl-CoA and the PduL reaction product that eluted at 10.9 min were at m/z = 824.1 or 824.2, respectively. These peaks correspond to $[M+H]^+$ for propionyl-CoA. In contrast, propionyl-CoA was undetectable by HPLC in assay mixtures containing cell extract from BE291 (Pta^- $PduL^-$) and the major HPLC peak observed corresponded to HS-CoA (retention time = 4.5 min). Our interpretation of the above results is that propionyl-CoA is a product of the PduL reaction.

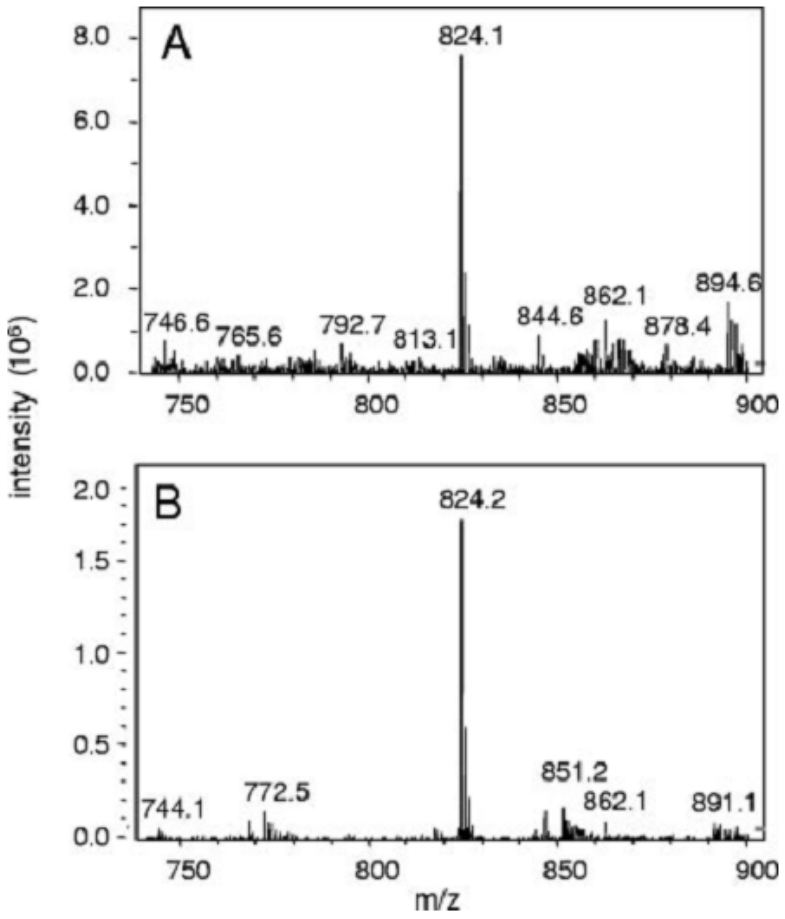

Fig. 7. Propionyl-CoA is produced by the PduL reaction. (A) HPLC-ESI-MS of propionyl-CoA standard. (B) HPLC-ESI-MS of a PduL assay after 10 min of incubation at 30°C. The assay mixture initially contained 10 µg cell extract from BE527 (Pta^- $PduL^+$), 0.4 mM HS-CoA, 1 mM propionyl- PO_4^{2-}, and buffer.

Production of PduL-his$_8$ Protein.

E. coli strain BE554 was constructed to produce high levels of recombinant PduL fused to 8 C-terminal histidine residues (PduL-his$_8$). Protein expression by BE554

and a control strain (BE119) were examined by SDS-PAGE (not shown) and enzyme assay. Relatively high amounts of a protein with a molecular mass near 27 kDa were present in the inclusion body fraction from the *pduL* expression strain, which is near the predicted molecular mass for PduL-his$_8$ (24 kDa). However, a modest amount of soluble protein near this mass was produced.

To better assess the production of PduL-His$_8$, cell extracts were tested for PTAC activity. Soluble extracts from the PduL production strain typically contained about 50 μmol min^{-1} mg^{-1} activity whereas the control strain produced only 2 μmol min^{-1} mg^{-1} PTAC activity. Hence, a reasonable amount of PduL-his$_8$ appeared to be soluble and active under the production conditions used. On the other hand, although the inclusion body fraction from the expression strain contained high amounts of PduL-his$_8$ protein, the PTAC activity of this fraction was typically about 2-fold lower than that of the soluble fraction indicating that most of the PduL in this fraction was inactive. No PTAC activity was detected in the inclusion body fraction from the control strain. The PTAC assay used measured the conversion of propionyl-PO_4^{2-} and HS-CoA to propionyl-CoA and HPO_4^{2-}. No activity could be detected when enzyme, HS-CoA or propionyl-PO_4^{2-} was omitted from the assay mixture. In each case, PTAC activity was linear with enzyme concentration (data not shown).

Purification and Kinetic Characterization of PduL-his$_8$.

PduL-his$_8$ was purified from cell extracts of strain BE554 by nickel-affinity chromatography (Fig. 8). Purified PduL-his$_8$ appeared homogenous following SDS-PAGE and staining Coomassie blue (Fig. 8). Kinetic analysis showed that purified PduL-his$_8$ was 3.8-fold more active with propionyl-PO_4^{2-} compared to

acetyl-PO_4^{2-} (V_{max} = 51.7 and 13.5 μmol min^{-1} mg^{-1}, respectively) (Table 3). It also had a lower K_m for propionyl-PO_4^{2-} than for acetyl-PO_4^{2-} (0.61±0.06 versus 0.97±0.26 mM). No activity was detected when PduL-his_8, HS-CoA or propionyl-PO_4^{2-} (or acetyl-PO_4^{2-}) was omitted from the assay mixture. In each case, the activity of PduL-his_8 activity was linear with enzyme concentration (data not shown).

For PduL-his_8, crude cell extracts typically had PTAC activity of about 50 μmol min^{-1} mg^{-1}. Nickel-affinity chromatography yielded purified enzyme with specific activities of about 45-55 μmol min^{-1} mg^{-1}. Visual inspection of SDS-PAGE gels indicated that PduL-his_8 comprised about 2-5% of the total cell protein (Fig 8); hence, these results suggest that PduL-his_8 lost activity during the course of purification. Indeed, PduL-his_8 was unstable in the purified form and lost about 50% of its activity 48 h after purification. The reported kinetic constants are based on assays done as soon as possible after purification. As the activity of PduL-his_8 decreased, its K_m for HS-CoA and propionyl-PO_4^{2-} remained unchanged within experimental error. Its activity with propionyl-PO_4^{2-} and acetyl-PO_4^{2-} decreased in direct proportion. We infer that the K_m values reported here are representative, but the V_{max} values are probably an underestimate.

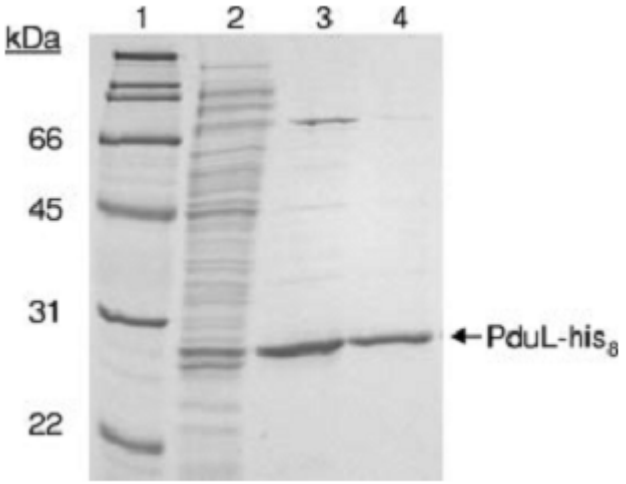

FIG. 8. SDS-PAGE analysis of PduL-His_8 purification. Lane1, molecular mass markers; lane 2, soluble crude extracts from the PduL-His_8 production strain (BE554) (10µg protein); lane 3, fraction obtained from the first elution step using buffer with 400 mM imidazole (2 µg protein); lane 4, fraction obtained from the second elution step using buffer with 400 mM imidazole (2 µg protein). A 12% acrylamide gel was stained with Coomassie brilliant blue R-250.

TABLE 3. Kinetic constants for purified recombinant PduL-His_8[a]

Substrate	K_m (mM)	V_{max} (µmol min^{-1} mg^{-1})	k_{cat} (s^{-1})	k_{cat}/K_m (mM s^{-1})
Propionyl-PO_4^{2-}	0.61 ± 0.06	51.7 ± 7.6	20.7	33.9
Acetyl-PO_4^{2-}	0.97 ± 0.26	13.4 ± 1.8	5.4	5.6

[a]PTAC assays were performed by monitoring the absorbance of reaction mixtures at 232 nm as described in Materials and Methods. The kinetic constants for propionyl-PO_4^{2-} and acetyl-PO_4^{2-} were determined using an excess of HS-CoA (0.4 mM).

Localization of PduL.

The pdu microcompartments pellet by high speed of centrifugation. Therefore, to localize PduL we measured for PTAC activity in the pellet and soluble fractions. We also tested phosphotransacylase activities in crude cell extracts, soluble proteins and the pellets for the *pta* null mutant (BE527) and several double mutants containing different *pdu* mutations (BE712, BE717, BE721, BE729, BE730) (Table 3). Compared with *pta* null mutant (BE527), *pta* and *pduJK* double mutant (BE721) had much lower percentage of PTAC activity in pellet. One reasonable interpretation of this was that PduL was associated with Pdu microcompartments through binding to shell protein PduJ or/and PduK. There was no significant difference in percentage of PduL activity in pellet between the *pta* null mutant (BE527) and either *pta* and *pduUT* double mutant (BE712), *pta* and *pduABB'* double mutant (BE717), *pta* and *pduP* double mutant (BE729) and *pta* and *pduW* double mutant (BE730). So it seemed unlikely that these shell proteins and enzymes involved in 1,2-PD degradation interacted with PduL.

Table 4. Phosphotransacylase activity in *pdu* mutants

Strain (relevant genotype)	PTAC activity (μmol min^{-1} mg^{-1})			Percentage of PduL activity in pelleted fraction
	Crude extract	s.n.	pellet	
BE527 (*pta*$^-$)	0.94	0.55	4.15±1.24	74.2±4.92%
BE712 (*pta*$^-$, *pduUT*$^-$)	2±0.1	0.7±0.15	5.18±0.94	63±1%
BE717 (*pta*$^-$, *pduABB'*$^-$)	4.83±1.03	0.8±0.25	4.49±0.26	56±9.83%
BE721 (*pta*$^-$, *pduJK*$^-$)	3.66±0.15	5.38±0.43	0.65±0.2	10.33±1.53%
BE729 (*pta*$^-$, *pduP*$^-$)	1.15	0.38	1.93	56%
BE730 (*pta*$^-$, *pduW*$^-$)	1.24	0.80	1.74	65%

Preparation of PduL-specific Antibody.

To determine the specificity of the polyclonal antibodies generated against the His_6-PduL protein, Western blots were performed on boiled cell lysates. Anti-PduL polyclonal antibodies recognized a specific protein band at 24 kDa in the wild-type strain but not in strain BE188 (which contains a nonpolar *pduL* deletion mutation) (Fig. 9, lanes 3 and 2). This indicated that the band at 24 kDa corresponded to the native PduL protein. Anti-PduL antibodies also recognized a protein band at 24 kDa in strain BE303 (Fig. 9, lane1), which carries a plasmid with the *pduL* gene.

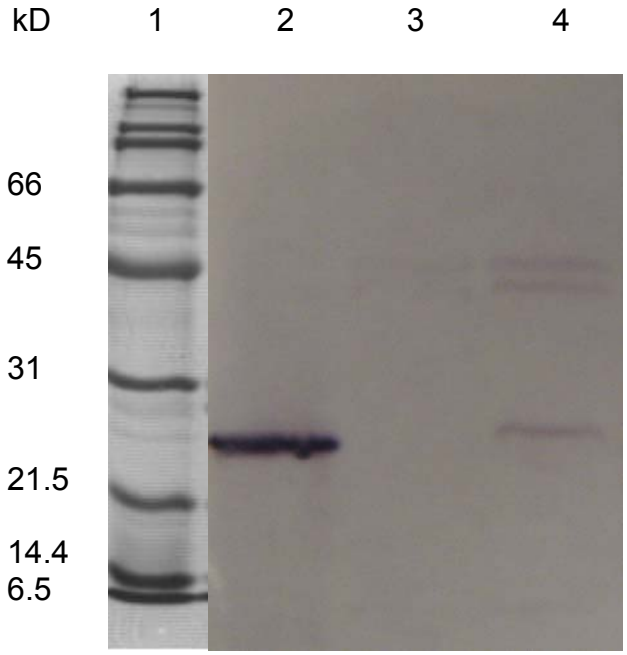

Fig. 9. Western analysis with anti-PduL polyclonal antibody preparations. Lane1, Molecular masses in kilodaltons, Lane 4, *S. enterica serovar Typhimurium* LT2; lane 3, BE188 (*pduL* mutant); lane 2, BE303 (PduL expression strain). Total protein loaded in lane 2 and lane 3 is 10 µg respectively, in lane 1 is 5 µg.

Western Blot Analysis of Purified Pdu Microcompartments.

To examine the presence of PduL protein in Pdu microcompartments, Western blots were performed on purified Pdu microcompartments from wildtype *Salmonella* strain LT2 using antisera against PduL protein. The antiserum specific for the PduL protein recognized a single band at 24 kDa (Fig. 10 lane 3). This is the expected value for PduL (23.1-kDa), indicating that this protein is a component of the purified microcompartments. Further, no specific band at 24 kDa was detected by Western blots perfomed on purified Pdu microcompartments from a nonpolar *pduL* deletion mutant.

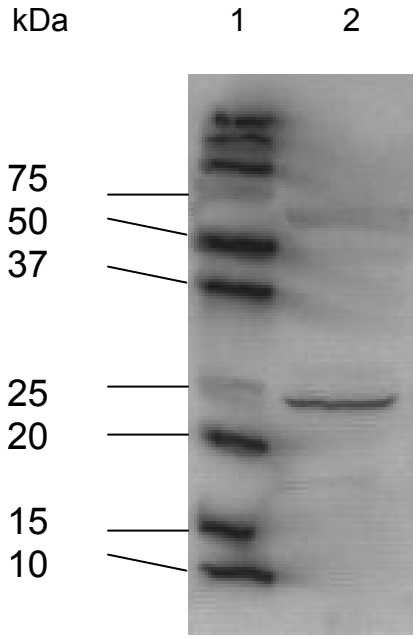

Fig. 10. Western blot analysis of purified Pdu microcompartments. Lane 1, molecular mass markers; lanes 2, 10 ug of purified Pdu microcompartments from *S. enterica serovar Typhimurium* LT2, probed with the anti-PduL antiserum.

Interactions between PduL and Other Pdu Microcompartments Proteins

To identify proteins that associate with PduL, we conducted a bacteria two-hybrid analysis of all the other genes from *pdu* operon using PduL as a bait. To construct the bait for the two-hybrid test, the PduL coding sequence was fused in frame to the full-length bacteriophage λ repressor protein (λcI, 237 amino acids), containing the amino-terminal DNA-binding domain and the carboxyl terminal dimerization domain. Each of the corresponding target proteins was fused to the N-terminal domain of the α-subunit of RNA polymerase (248 amino acids) and vice versa, i.e. the coding sequence of each other 20 genes from *pdu* operon was fused in frame to the full-length bacteriophage λ repressor protein and PduL as target was fused to the N-terminal domain of the α-subunit of RNA polymerase (Fig.11). Prior to performing a two-hybrid analysis, we determined whether the bait fusion protein was capable of activation of the reporter cassette in the absence of an interaction partner. To do this self-activation test, the BacterioMatch II reporter strain is cotransformed with the recombinant pBT plasmid and the empty pTRG vector. We also did the self activation test for all recombinant pTRG constructs. The data showed that cotransformation pair for all recombinant pBT plasmid didn't produce a significant number of colonies on selective screening medium (5 mM 3-AT), which meant the baits were suitable for use in the BacterioMatch II two-hybrid system. Some of the self tests for the target constructs including pTRG-*pduB'*, pTRG-*pduC*, pTRG-*pduH* and pTRG-*pduS* showed growth of some colonies, and we must considered in explanation of the later tests. The activation of HIS3 reporter gene and a second reporter streptomycin resistance gene aadA were used to select for protein-protein interactions. The

two-hybrid tests performed on selective screening medium (5mM 3-AT) showed a significant number of colonies for the pair PduL and PduB', PduL and PduD, PduL and PduM, PduL and PduN, PduL and PduW, PduL and PduX as shown in Table 4. Positive colonies were confirmed by testing their growth on dual selective medium (5mM 3-AT and streptomycin).

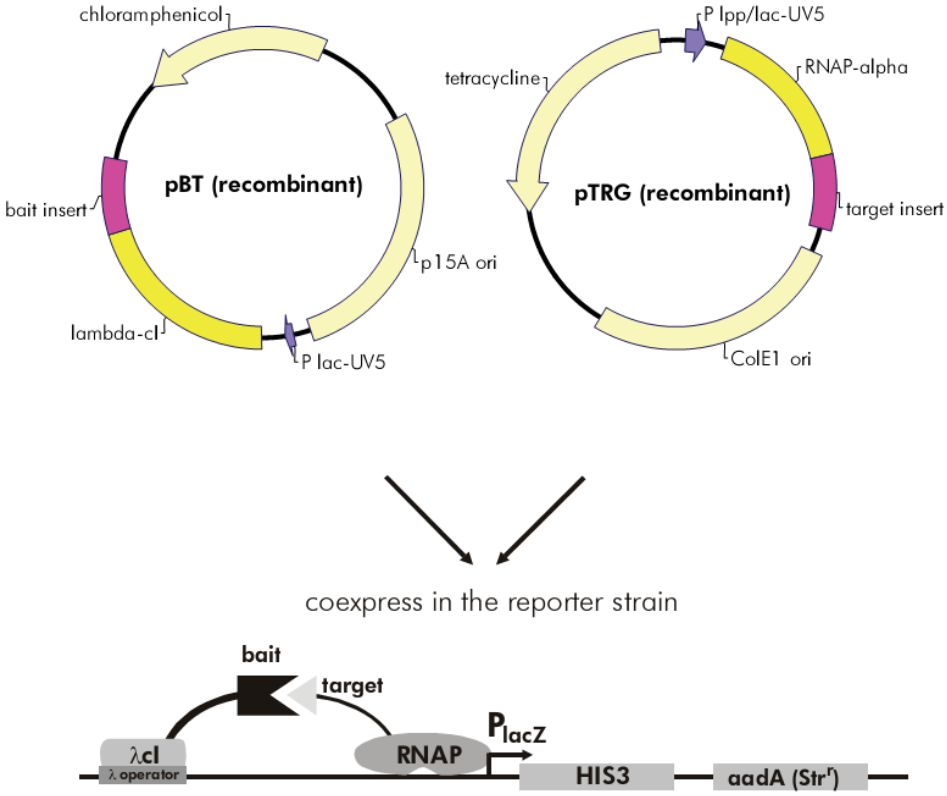

Fig.11. Construction of bait and target recombinant plasmids and the schematic of the BacterioMatch II two-hybrid system (Stratagene) dual reporter construct.

Table. 5A. Two-hybrid test for pBT/*pduL* and each of other Pdu proteins

	pBT/pduL			*pBT/pduL*	
	NS[a]	S[b]		NS	S
pTRG/pduA	2	0	*pTRG/pduM*	240	3
pTRG/pduB'	17	0	*pTRG/pduN*	TNTC	7
pTRG/pduBB'	420	1	*pTRG/pduO*	18	0
pTRG/pduC	TNTC[c]	1	*pTRG/pduP*	N/D	N/D
pTRG/pduD	85	1	*pTRG/pduQ*	TNTC	1
pTRG/pduE	lawn	2	*pTRG/pduS*	lawn	5
pTRG/pduG	TNTC	5	*pTRG/pduT*	70	0
pTRG/pduH	N/D[d]	N/D	*pTRG/pduU*	30	0
pTRG/pduJ	500	0	*pTRG/pduV*	80	1
pTRG/pduK	TNTC	0	*pTRG/pduW*	lawn	0
pTRG/pduJK	300	1	*pTRG/pduX*	160	1

[a]Average colony numbers grown on each nonselective medium plate from 100ul aliquots of 1:100 diluted cotransformation mixture.
[b]Average colony numbers grown on each selective medium plate (5mM 3-AT) from 100ul aliquots of cotransformation mixture.
[c]Too numerous to count.
[d]Not done.

Table. 5B. Two-hybrid test for pTRG/*pduL* and each of other Pdu proteins

	pTRG/pduL			*pTRG/pduL*	
	NS[a]	S[b]		NS	S
pBT/pduA	100	0	*pBT/pduM*	lawn	97
pBT/pduB'	lawn	430	*pBT/pduN*	lawn	240
pBT/pduBB'	N/D[d]	N/D	*pBT/pduO*	TNTC[c]	44
pBT/pduC	lawn	6	*pBT/pduP*	10	0
pBT/pduD	lawn	450	*pBT/pduQ*	140	0
pBT/pduE	lawn	3	*pBT/pduS*	TNTC	3
pBT/pduG	N/D	N/D	*pBT/pduT*	20	0
pBT/pduH	lawn	5	*pBT/pduU*	TNTC	0
pBT/pduJ	15	0	*pBT/pduV*	lawn	1
pBT/pduK	N/D	N/D	*pBT/pduW*	lawn	120
pBT/pduJK	lawn	4	*pBT/pduX*	lawn	600

[a]Average colony numbers grown on each nonselective medium plate from 100ul aliquots of 1:100 diluted cotransformation mixture.
[b]Average colony numbers grown on each selective medium plate (5mM 3-AT) from 100ul aliquots of cotransformation mixture.
[c]Too numerous to count.
[d]Not done.

DISCUSSION

Here we presented genetic and biochemical evidence that the *pduL* gene encodes a PTAC involved in 1,2-PD degradation. Growth tests showed that a *pduL* mutant was impaired for 1,2-PD degradation under aerobic and anaerobic conditions indicating a role for *pduL* in 1,2-PD degradation. Growth studies also showed that ectopic expression of PduL corrected the growth defect of a *pta* mutant on acetate minimal medium indicating that PduL has phosphotransacetylase activity in vivo. Enzyme assays of crude cell extracts demonstrated that *pduL* was necessary for the production of detectable PTAC activity in a genetic background that contained a *pta* mutation. HPLC-ESI-MS showed that propionyl-CoA was produced from propionyl-PO_4^{2-} and HS-CoA in PduL enzyme assays. PduL-his_8 was purified and found to have a specific activity of 57.4 μmol min^{-1} mg^{-1} with propionyl-PO_4^{2-} as substrate indicating the PduL is sufficient for PTAC activity. Thus, genetic and biochemical studies indicate that PduL is a PTAC involved in 1,2-PD degradation.

Blast and PSI-Blast analyses (5 iterations) showed that PduL lacks significant similarity to known PTAC enzymes. Thus, PduL is evolutionarily distinct. It either evolved independently of known PTAC enzymes or it became highly divergent from them over time. Sequence analyses also showed that PduL homologues (expect $<7x10^{-30}$) are found in 49/337 (14.5%) complete microbial genomes present in GenBank. No homologues of PduL were found among the Archaea or Eukarya. Hence, PduL is apparently a conserved protein specific to the Bacteria. In addition, Blast analyses identified 4 PduL homologues that are fused to sequences with

homology to acetate kinases. These may be dual function enzymes that convert acyl-CoA to its corresponding organic acid with the synthesis of ATP.

Including PduL, there are three known classes of phosphotransacylases. The *S. enterica* PduL, Pta, and EutD enzymes are representatives of these classes. PduL is comprised of 210 amino acids while Pta and EutD are 714 and 338 amino acids in length, respectively (8). EutD and the C-terminal region of Pta are homologous. PduL lacks significant similarity to EutD and Pta. The N-terminal region of Pta contains BioD-like and "DRTGG" domains. These two domains are absent from EutD and PduL. The physiological role of these domains is uncertain. In enterica bacteria, acetyl-group metabolism and is linked to two-component signal transduction systems and DNA damage and repair in a complex manner (22, 34, 40). The N-terminal domains of Pta may be needed to accommodate expanded physiological roles.

Kinetic studies were performed with purified PduL-his$_8$ (Table 3). The V_{max} of PduL with propionyl-PO_4^{2-} as substrate was 51.7±7.6 μmol min^{-1} mg^{-1}. Previously purified Pta enzymes were reported to have specific activities between 32 and 9006 μmol min^{-1} mg^{-1} when an acyl-PO_4^{2-} was used as substrate (33). The activity of PduL-his$_8$ is at the low end of this range, but may be an underestimate due to its instability (see results section).

The K_m values of PduL-his$_8$ for HS-CoA and propionyl-PO_4^{2-} were determined to be 0.61±0.06 and 0.032±0.006 mM, respectively. Reported K_m values of Pta homologues for HS-CoA range from 0.03 to 1.7 mM and for acetyl-PO_4^{2-} range from 0.024 to 4.7 mM (33). Thus, K_m values of PduL for HS-CoA and propionyl-PO_4^{2-} appear to be within a physiologically meaningful range. Kinetic studies found that

K_{cat}/K_m of Pdu-his_8 was about 6-fold higher for propionyl-PO_4^{2-} compared to acetyl-PO_4^{2-}. The selectivity of PduL for propionyl-PO_4^{2-} is consistent with a role in 1,2-PD degradation. Furthermore, its relatively low activity with acetyl-PO_4^{2-} may be important to minimize perturbation of acetyl-group metabolism (22, 40).

Two findings in this report were surprising to us: 1) the observation that *pduL* mutants were significantly impaired for growth on 1,2-PD minimal medium (Fig. 6) and 2) the finding that a *pduL pta* double mutant was not further impaired for growth on 1,2-PD. Because Pta is known to be active with propionyl-PO_4^{2-}, we expected that Pta would partly substitute for PduL during growth of *S. enterica* on 1,2-PD. However, in the studies reported here, it did not. A simple explanation is that PduL is more efficient at propionyl-group metabolism in vivo. Two explanations we think are more interesting are differential regulation of *pta* and *pduL*, as well as the possibility that PduL is specifically adapted to function in concert with the microcompartment involved in 1,2-PD degradation.

The demonstration of PduL as an distinct phosphotransacylase which participates in degradation of 1,2-PD in *Salmonella* opened several interesting questions, namely: Is PduL one of the components of Pdu microcompartments in *Salmonella*? How does PduL interact with Pdu microcompartments? Which protein(s) from Pdu microcompartments act as binding partners for PduL protein? And why does PduL bind to Pdu microcompartments? Here we tried several ways to investigate the relationship between PduL protein and Pdu microcompartments.

In the previous studies by Gregory D. Havemann and Thomas A. Bobik (14), N-terminal sequencing, and protein mass fingerprinting via matrix-assisted laser

desorption ionization–time-of-flight mass spectrometry (MALDI-TOF MS) identified at least 15 proteins including PduABB'CDEGHJKOPTU in Pdu microcompartments. PduL was not identified to be part of Pdu microcompartments in that study. However, the theoretical isoelectric point (pI) for PduL is 9.09 so it may have accumulated at the edge of two-dimensional electrophoresis gel from which the 15 spots were identified as the proteins in Pdu microcompartments. Preliminary data showed PduL enzyme activity in the pelleted crude cell extract (containing Pdu microcompartments) accounted for more than 50% of all the PTAC activity. This indicated that PduL was associated with Pdu microcompartments. Here, our immunoblot analysis for purified Pdu microcompartments indicated that PduL was indeed part of Pdu microcompartments.

There are 23 genes in *pdu* locus of *Salmonella* (6, 7, 10), PduL might associate with any of shell proteins or enzymes in the microcompartments. PduL enzyme assays for several Pdu microcompartments shell proteins mutants showed that *pduJK* mutant had much lower percentage of PduL activity in pelleted fraction rather than soluble fraction of cell crude extracts. The results indicated PduJK provided binding sites for PduL. To further investigate interactions between PduL and other Pdu proteins, we performed bacterial two-hybrid analysis. Several proteins including PduB', PduD, PduM, PduN, PduW and PduX were isolated as candidate binding partners of PduL. PduB' is the truncated version of PduB lacking N-terminal 37 amino acids. N-terminal sequencing and protein mass fingerprinting both identified it as part of Pdu microcompartments (14), and it was distantly related to Csos1, a shell protein of carboxysome *H. neapolitanus* (6, 67, 68), so it may serve as a shell component.

Hence, it is possible that PduL associated with Pdu microcompartments through binding to the shell protein PduB'. PduD is medium subunit of coenzyme B_{12}-dependent diol dehydratase, it may interacted somehow with PduL since they both catalyze the degradation of 1,2-PD. Up to now we still don't know the functions of PduM, *S. enterica* strains with deletions of the *pduM* gene form abnormal microcompartments suggesting that the PduM protein may play a structural role (84). If so, PduM might also contain binding domain or motif for PduL protein. PduN was a protein with homology to the pentamer proposed to form the carboxysome vertices. Based on homology to carboxysomes, the shell of the Pdu microcompartments may have faces made from PduA and PduJ hexamers and vertices made from PduN pentamers (85). Propionate kinase PduW was undetectable in the purified Pdu microcompartments indicating that it might function in the cytoplasm of the cell (14). Since the substrate of PduW is propionyl-PO_4^{2-}, the product from the reaction catalyzed by PduL, we thought it was possible that PduL and PduW interact with each other so that the conversion of propionyl-CoA to propionate could performed more efficiently and faster. If so, PduL might either localize close to the shell inside of Pdu microcompartments and stick out through the holes in the shell and provide propionyl-PO_4^{2-} to PduW, or be located near outside of the shell where it associated with microcompartments through binding to some shell components like PduB' or PduN and interacted with PduW in the cytoplasm of the cell.

CONCLUSIONS AND FUTURE DIRECTIONS

The findings by earlier enzymatic analysis that a PTAC was used for 1,2-PD degradation while the enzyme involved was not determined triggered interest in identifying this enzyme. This dissertation puts emphasis on elucidating the protein encoded by the *pduL* gene which acts as a conserved evolutionarily distinct PTAC in 1,2-PD degradation by *S. enterica*.

Genetic and Biochemical Evidence of PduL in 1,2-PD Degradation

The first part of this study presented genetic and biochemical evidence that the *pduL* gene encodes a PTAC involved in 1,2-PD degradation. Previous immunoelectron microscopy and DNA sequence analysis already identified most of the enzymes needed for 1,2-PD degradation, which are coenzyme B_{12}-dependent diol dehydratase (PduCDE), propionaldehyde dehydrogenase (PduP), propionate kinase (PduW), and 1-propanol dehydrogenase (PduQ) (6). Here we identified the phosphotransacylase was involved in 1,2-PD degradation.

Tests with MacConkey–1,2-PD medium of independent *pduL* deletion mutants showed less acid produced from degradation of propanediol. Growth tests indicated impaired aerobic growth on 1,2-PD for *pduL* mutants and energy production via 1,2-PD fermentation was completely eliminated by the *pduL* mutation. These all suggested a role for PduL in 1,2-PD degradation. Further, complementation studies were conducted to demonstrate that the aerobic and anaerobic growth phenotypes were fully corrected by the expression of a *pduL* minimal clone.

There are three known classes of phosphotransacylases in *S. enterica*. Among them, EutD enzyme is only expressed under specific conditions other than growth

under 1,2-PD. Enzyme assays demonstrated that both PduL and Pta contained PTAC activities and indicated PduL was more likely to function in 1,2-PD degradation while Pta worked better for acetyl group metabolism (20). Next, HPLC-ESI-MS showed that propionyl-CoA was a product of the PduL reaction. Kinetic analysis of purified PduL-His_8 showed that it was 3.8-fold more active with propionyl-PO_4^{2-} than with acetyl- PO_4^{2-}. So genetic and biochemical studies indicate that PduL is a PTAC involved in 1,2-PD metabolism pathway.

PduL is a Component of Pdu Microcompartments and Associate with Pdu Proteins

The second part of this study investigated the relationship between PduL and Pdu microcompartments. Our previous unpublished studies showed most of PduL activity was present with microcompartments in cell crude extract. This data together with the above results raised our interest localizating PduL protein in *S. enterica*.

His_8-PduL protein was obtained from Ni^{2+} affinity chromatography and used for production of anti-PduL antiserum. *S. enterica*. The Pdu microcompartments were purified by way of lysozyme, B-per II bacterial protein extraction reagent and centrifugation. Western blot for purified Pdu microcompartments using anti-PduL antibody demonstrated that PduL was a component of Pdu microcompartments.

PduL enzyme assays and bacterial two-hybrid screens were used to investigate the possible interactions between PduL and other proteins from Pdu microcompartments. We analyzed phosphotransacylase activity in several double mutants and found that PduJ or PduK could be candidates interacting with PduL.

Bacterial two-hybrid analysis identified PduB', PduM, PduN, and PduW as possible proteins which may act as binding partners for PduL.

Future Experimentation

Here in this study, enzyme assays suggested that PduL might be part of Pdu microcompartments and interact with some Pdu microcompartment shell components. Western blot indicated that PduL is associated with microcompartment, and bacterial two-hybrid analysis suggested some possible partner proteins for PduL. Further tests are needed to confirm and identify the complicated relationship between PduL protein and Pdu microcompartments.

At present, we do not know why PduL is associated with Pdu microcompartments. But we know that coenzyme A is required for the degradation of 1,2-PD. The mechanisms by which molecules like coenzyme A, cobalamin B_{12} and to pass through the protein shell and go into the microcompartments are currently unknown. One possibility is that coenzyme A enters the microcompartments during the formation of the Pdu microcompartments. If so, coenzyme A will be consumed during the degradation process and need to be recycled. The reaction by PduL regenerates coenzyme A from propionyl-CoA, so PduL may help in the coenzyme A recycling. Pantothenic acid, also called vitamin B5, is a water-soluble vitamin which is needed to form coenzyme A. Mutation of pantothenic acid encoding gene prevents bacteria from synthesizing coenzyme A, then we could control the amount of coenzyme A within cells by adding certain amount of pantothenic acid to the growth medium. And this model will be helpful in detecting the interaction between PduL and coenzyme A recycling.

ACKNOWLEDGMENTS

I would like to thanks my mentor Dr. Thomas Bobik for his help, guidance and support over the past four years. His dedication to research in science always touched and inspired me and his great sense of humor always cheered me up. He introduced basic and advanced knowledge in bacterial genetics to me and went through many experiments together with me. He paid full respects to ideas and decisions of his graduate students which I truly appreciated.

I would like to thank the rest of my committee: Dr. Louisa Tabatabai, whose advice on protein chemistry greatly facilitated my research; Dr. Qijing Zhang, whose advice on methods in protein-protein interactions opened my eyes in the subfield; and Dr. Kenneth Koehler, whose great knowledge and experience in Statistics turned me on to the invigorating combination of biological sciences with statistical analysis.

I am grateful to the personnel of the Protein facility at Iowa State University who performed the internal peptide digestion-sequencing, Joel Nott gave me instructions about 2D-PAGE; Siquan Luo from Proteomics facility at Iowa State University performed mass spectrometry.

Special thanks go to my parents and my brother, whose support was critical to help me go through a series of difficulties and complete my studies here.

My thanks also go to Shouqiang Cheng and Chenguang Fan. Shouqiang's experience in biology and Chenguang's techniques in protein purification and analysis helped me a lot.

REFERENCES

1. **Abeles, R. H., and H. A. Lee.** 1961. Intramolecular oxidation-reduction requiring a cobamide coenzyme. J. Biol. Chem. **236:**2347-2350.
2. **Altschul, S. F., T. L. Madden, A. A. Schaffer, J. Zhang, Z. Zhang, W. Miller, and D. J. Lipman.** 1997. Gapped BLAST and PSI-BLAST: a new generation of protein database search programs. Nucleic Acids Res. **25:**3389-3402.
3. **Berkowitz, D., J. M. Hushon, H. J. Whitfield, Jr., J. Roth, and B. N. Ames.** 1968. Procedure for identifying nonsense mutations. J. Bacteriol. **96:**215-220.
4. **Bobik, T. A.** 2006. Polyhedral organelles compartmenting bacterial metabolic processes. Appl. Microbiol. Biotechnol. **70:**517-525.
5. **Bobik, T. A., M. Ailion, and J. R. Roth.** 1992. A single regulatory gene integrates control of vitamin B_{12} synthesis and propanediol degradation. J. Bacteriol. **174:**2253-2266.
6. **Bobik, T. A., G. D. Havemann, R. J. Busch, D. S. Williams, and H. C. Aldrich.** 1999. The propanediol utilization (*pdu*) operon of *Salmonella enterica* serovar Typhimurium LT2 includes genes necessary for formation of polyhedral organelles involved in coenzyme B_{12}-dependent 1,2-propanediol degradation. J. Bacteriol. **181:**5967-5975.
7. **Bobik, T. A., Y. Xu, R. M. Jeter, K. E. Otto, and J. R. Roth.** 1997. Propanediol utilization genes (*pdu*) of *Salmonella typhimurium*: three genes for the propanediol dehydratase. J. Bacteriol. **179:**6633-6639.
8. **Brinsmade, S. R., and J. C. Escalante-Semerena.** 2004. The eutD gene of *Salmonella enterica* encodes a protein with phosphotransacetylase enzyme activity. J. Bacteriol. **186:**1890-1892.
9. **Brinsmade, S. R., T. Paldon, and J. C. Escalante-Semerena.** 2005. Minimal functions and physiological conditions required for growth of *Salmonella enterica* on ethanolamine in the absence of the metabolosome. J. Bacteriol. **187:**8039-8046.
10. **Chen, P., D. I. Andersson, and J. R. Roth.** 1994. The control region of the *pdu/cob* regulon in *Salmonella typhimurium*. J. Bacteriol. **176:**5474-5482.
11. **Datsenko, K. A., and B. L. Wanner.** 2000. One-step inactivation of chromosomal genes in *Escherichia coli* K-12 using PCR products. Proc. Natl. Acad. Sc.i U S A **97:**6640-6645.
12. **Davis, R. W., D. Botstein, and J. R. Roth.** 1980. Advanced bacterial genetics: a manual for genetic engineering. Cold Spring Harbor Laboratory, Cold Spring Harbor, N.Y.
13. **Dawson, R. M. C., D. C. Elliott, W. H. Elliott, and K. M. Jones (ed.).** 1969. Data for biochemical research, 2nd ed. Oxford University Press, Oxford.
14. **Havemann, G. D., and T. A. Bobik.** 2003. Protein content of polyhedral organelles involved in coenzyme B_{12}-dependent degradation of 1,2-propanediol in *Salmonella enterica* serovar Typhimurium LT2. J. Bacteriol. **185:**5086-5095.
15. **Havemann, G. D., E. M. Sampson, and T. A. Bobik.** 2002. PduA is a shell protein of polyhedral organelles involved in coenzyme B_{12}-dependent degradation of 1,2-propanediol in *Salmonella enterica* serovar Typhimurium LT2. J. Bacteriol. **184:**1253-1261.

16. **Horswill, A., and J. Escalante-Semerena.** 1997. Propionate catabolism in *Salmonella typhimurium* LT2: two divergently transcribed units comprise the *prp* locus at 8.5 centisomes, *prpR* encodes a member of the sigma-54 family of activators, and the *prpBCDE* genes constitute an operon. J. Bacteriol. **179:**928-940.
17. **Jeter, R. M.** 1990. Cobalamin-dependent 1,2-propanediol utilization by *Salmonella typhimurium*. J. Gen. Microbiol. **136:**887-986.
18. **Johnson, C. L., E. Pechonick, S. D. Park, G. D. Havemann, N. A. Leal, and T. A. Bobik.** 2001. Functional genomic, biochemical, and genetic characterization of the *Salmonella pduO* gene, an ATP:cob(I)alamin adenosyltransferase gene. J. Bacteriol. **183:**1577-1584.
19. **Leal, N. A., G. D. Havemann, and T. A. Bobik.** 2003. PduP is a coenzyme A-acylating propionaldehyde dehydrogenase associated with the polyhedral bodies involved in B_{12}-dependent 1,2-propanediol degradation by *Salmonella enterica* serovar Typhimurium LT2. Arch. Microbiol. **180:**353-361.
20. **LeVine, S. M., F. Ardeshir, and G. F. Ames.** 1980. Isolation and characterization of acetate kinase and phosphotransacetylase mutants of *Escherichia coli* and *Salmonella typhimurium*. J. Bacteriol. **143:**1081-1085.
21. **Lundie, L. L., Jr., and J. G. Ferry.** 1989. Activation of acetate by *Methanosarcina thermophila*. J. Biol. Chem. **264:**18392-18396.
22. **McCleary, W. R., J. B. Stock, and A. J. Ninfa.** 1993. Is acetyl phosphate a global signal in *Escherichia coli*? J. Bacteriol. **175:**2793-2798.
23. **Miller, J. H.** 1972. Experiments in molecular genetics. Cold Spring Harbor Laboratory, Cold Spring Harbor, N.Y.
24. **Miller, V. L., and J. J. Mekalanos.** 1988. A novel suicide vector and its use in construction of insertion mutations: osmoregulation of outer membrane proteins and virulence determinants in *Vibrio cholerae* requires *toxR*. J. Bacteriol. **170:**2575-2583.
25. **Obradors, N., J. Badia, L. Baldoma, and J. Aguilar.** 1988. Anaerobic metabolism of the L-rhamnose fermentation product 1,2-propanediol in *Salmonella typhimurium*. J. Bacteriol. **170:**2159-2162.
26. **Palacios, S., V. J. Starai, and J. C. Escalante-Semerena.** 2003. Propionyl coenzyme A is a common intermediate in the 1,2-propanediol and propionate catabolic pathways needed for expression of the *prpBCDE* operon during growth of *Salmonella enterica* on 1,2-propanediol. J. Bacteriol. **185:**2802-2810.
27. **Paoli, P., P. Cirri, L. Camici, G. Manao, G. Cappugi, G. Moneti, G. Pieraccini, G. Camici, and G. Ramponi.** 1997. Common-type acylphosphatase: steady-state kinetics and leaving-group dependence. Biochem. J. **327:**177-184.
28. **Penrod, J. T., and J. R. Roth.** 2006. Conserving a volatile metabolite: a role for carboxysome-like organelles in *Salmonella enterica*. J. Bacteriol. **188:**2865-2874.
29. **Price-Carter, M., J. Tingey, T. A. Bobik, and J. R. Roth.** 2001. The alternative electron acceptor tetrathionate supports B_{12}-dependent anaerobic growth of *Salmonella enterica* serovar Typhimurium on ethanolamine or 1,2-propanediol. J. Bacteriol. **183:**2463-2475.
30. **Sambrook, J., E. F. Fritsch, and T. Maniatis.** 1989. Molecular cloning: a laboratory manual, 2nd ed. Cold Spring Harbor Laboratory, Cold Spring Harbor, N.Y.

31. **Sampson, E. M., C. L. Johnson, and T. A. Bobik.** 2005. Biochemical evidence that the *pduS* gene encodes a bifunctional cobalamin reductase. Microbiology **151:**1169-1177.
32. **Schmieger, H.** 1971. A method for detection of phage mutants with altered transducing ability. Mol. Gen. Genet. **110:**378-381.
33. **Schomburg, I., A. Chang, C. Ebeling, M. Gremse, C. Heldt, G. Huhn, and D. Schomburg.** 2004. BRENDA, the enzyme database: updates and major new developments. Nucleic Acids Res. **32:**D431-433.
34. **Shi, I. Y., J. Stansbury, and A. Kuzminov.** 2005. A defect in the acetyl coenzyme A<-->acetate pathway poisons recombinational repair-deficient mutants of *Escherichia coli*. J. Bacteriol. **187:**1266-1275.
35. **Shimizu, M., T. Suzuki, K. Y. Kameda, and Y. Abiko.** 1969. Phosphotransacetylase of *Escherichia coli* B, purification and properties. Biochim. Biophys. Acta. **191:**550-558.
36. **Shively, J. M., C. E. Bradburne, H. C. Aldrich, T. A. Bobik, J. L. Mehlman, S. Jin, and S. H. Baker.** 1998. Sequence homologs of the carboxysomal polypeptide CsoS1 of the thiobacilli are present in cyanobacteria and enteric bacteria that form carboxysomes - polyhedral bodies. Can. J. Bot. **76:**906-916.
37. **Toraya, T., S. Honda, and S. Fukui.** 1979. Fermentation of 1,2-propanediol and 1,2-ethanediol by some genera of *Enterobacteriaceae*, involving coenzyme B_{12}-dependent diol dehydratase. J. Bacteriol. **139:**39-47.
38. **Vogel, H. J., and D. M. Bonner.** 1956. Acetylornithinase of *Escherichia coli*: partial purification and some properties. J. Biol. Chem. **218:**97-106.
39. **Warren, J. W., J. R. Walker, J. R. Roth, and E. Altman.** 2000. Construction and characterization of a highly regulable expression vector, pLAC11, and its multipurpose derivatives, pLAC22 and pLAC33. Plasmid **44:**138-151.
40. **Wolfe, A. J., D. E. Chang, J. D. Walker, J. E. Seitz-Partridge, M. D. Vidaurri, C. F. Lange, B. M. Pruss, M. C. Henk, J. C. Larkin, and T. Conway.** 2003. Evidence that acetyl phosphate functions as a global signal during biofilm development. Mol. Microbiol. **48:**977-988.
41. **JR Roth, JG Lawrence, and TA Bobik.** 1996. Cobalamin (Coenzyme B12): Synthesis and Biological Significance. Annu. Rev. Microbiol. 50:137–81.
42. **Lawrence JG, Roth JR.** 1995. Evolution of coenzyme B_{12} synthesis among enteric bacteria: evidence for loss and reacquisition of a multigene complex. Genetics. 142:11–24.
43. **N Obradors, J Badía, L Baldomà and J Aguilar J.** 1988. Anaerobic metabolism of the L-rhamnose fermentation product 1,2- propanediol in Salmonella typhimurium. J.Bacteriol.170:2159–62.
44. **Lin ECC.** 1987. Dissimilatory pathways for sugars, polyols, and carboxylates. In Escherichia coli and Salmonella typhimurium: Cellular and Molecular Biology, ed. FD Niedhardt, JL Ingraham, KB Low, B Magasanik, M Schaechter, HE Umbarger, pp. 244–84. Washington, DC: Am. Soc. Microbiol.
45. **BradbeerC.** 1965. The clostridial fermentations of choline and ethanolamine. I. Preparation and properties of cell-free extracts.J.Biol. Chem.240:4669–74.

46. **Scarlett FA, Turner JM.** 1976. Microbial metabolism of amino alcohols. Ethanolamine catabolism mediated by coenzyme B_{12}-dependent ethanolamine ammonia-lyase in *Escherichia coli* and *Klebsiella aerogenes*. J. Gen. Microbiol. 95:173–76.
47. **Forage RG, Foster MA.** 1982. Glycerol fermentation in Klebsiella pneumoniae: functions of the coenzyme B_{12}-dependent glycerol and diol dehydratases. J. Bacteriol.149:413–19.
48. **Jeter R, Olivera BM, Roth JR.** 1984. *Salmonella typhimurium* synthesizes cobalamin (vitamin B_{12}) de novo under anaerobic growth conditions. J. Bacteriol. 159:206–16.
49. **Jeter RM, Roth JR.** 1987. Cobalamin (vitamin B_{12}) biosynthetic genes of *Salmonella typhimurium*. J. Bacteriol. 169:3189–98.
50. **Roth JR, Lawrence JG, Rubenfield M, Kieffer-Higgins S, Church GM.** 1993. Characterization of the cobalamin (vitamin B_{12}) biosynthetic genes of *Salmonella typhimurium.* J. Bacteriol. 175:3303–16.
51. **Van Dyk TK, LaRossa RA.** 1987. Involvement of *ack-pta* operon products in α-ketobutyrate metabolism by *Salmonella typhimurium*. Mol. Gen. Genet. 207: 435–40
52. **Michael Ailion, Thomas A. Bobik, and John R. Roth.** 1993. Two Global Regulatory Systems (Crp and Arc) Control the Cobalamin/Propanediol Regulon of Salmonella typhimurium. J. Bacteriol. 175: 7200-08.
53. **Chen P, Ailion M, Bobik T, Stormo G, Roth J.** 1995. Five promoters integrate control of the *cob/pdu* regulon in *Salmonella typhimurium*. J. Bacteriol. 177:5401–10.
54. **Bobik TA.** 2007. Bacterial microcompartments. Microbe 2:25–31.
55. **Cannon GC, Bradburne CE, Aldrich HC, Baker SH, Heinhorst S, et al.** 2001. Microcompartments in prokaryotes: carboxysomes and related polyhedra. Appl Environ Microbiol 67:5351–6361.
56. **Kerfeld CA, Sawaya MR, Tanaka S, Nguyen CV, Phillips M, et al.** 2005. Protein structures forming the shell of primitive bacterial organelles. Science 309:936–938.
57. **Shively JM, Ball F, Brown DH, Saunders RE.** 1973. Functional organelles in prokaryotes: polyhedral inclusions (carboxysomes) of *Thiobacillus neapolitanus*. Science 182:584–586.
58. **Price GD, Badger MR, Woodger FJ, Long BM.** 2007. Advances in understanding the cyanobacterial CO2-concentrating-mechanism (CCM): functional components, Ci transporters, diversity, genetic regulation and prospects for engineering into plants. J Exper Bot Advance accesss DOI: 10.1093/jxb/erm112.
59. **Drews G, Niklowitz W.** 1956. Beitrage zur Cytologie der Blaualgen. II. Zentroplasma und18 granulare Einschlusse von Phormidium uncinatum. Arch Mikrobiol 24:147–162.
60. **Kaplan A, Reinhold L.** 1999. CO_2 concentrating mechanisms in photosynthetic microorganisms. Ann Rev of Plant Physiol and Plant Mol Biol 50:539–570.
61. **Shively JM, van Keulen G, Meijer WG.** 1998. Something from almost nothing: carbon dioxide fixation in chemoautotrophs. Ann Rev Microbiol 52:191–230.

62. **Yeates TO, Tsai Y, Tanaka S, Sawaya MR, Kerfeld CA.** 2007. Self- assembly in the carboxysome: aviral capsid-like protein shell in bacterial cells. Biochem Soc Trans 35:508–511.
63. **Tanaka S, Kerfeld CA, Sawaya MR, Cai F, Heinhorst S, et al.** 2008. Atomic-level models of the bacterial carboxysome shell. Science 319:1083–1086.
64. **Fukuzawa H, Suzuki E, Komukai Y, Miyachi S.** 1992. A gene homologous to chloroplast carbonic anhydrase (icfA) is essential to photosynthetic carbon dioxide fixation by Synechococcus PCC7942. ProcNatl AcadSci USA 89:4437–4441.
65. **Reinhold L, Kosloff R, Kaplan A.** 1991. A model for inorganic carbon fluxes and photosynthesis in cyanobacterial carboxysomes. Canadian Journal of Botany-Revue Canadienne De Botanique 69:984–988.
66. **Reinhold L, Zviman M, Kaplan A**, editors. 1987. Inorganic carbon fluxes and photosynthesis in cyanobacteria: a quantitative model. Dordrecht: Martinus Nijhoff. pp 289–296.
67. **Cannon GC, Shively JM.** 1983. Characterization of a homogenous preparation of carboxysomes from Thiobacillus neapolitanus. Arch Microbiol 134:52–59.
68. **Holthuijzen YA, Breemen JFL, Kuenen GJ, Konings WN.** 1986. Protein composition of the carboxysomes of Thiobacillus neapolitanis. Arch Microbiol 144:398–404.
69. **Baker SH, Lorbach SC, Rodriguez-Buey M, Williams DS, Aldrich HC**, et al. 1999. The correlation of the gene csoS2 of the carboxysome operon with two polypeptides of the carboxysome in *Thiobacillus neapolitanus*. Arch Microbiol 172:233–239.
70. **Badger MR, Hanson D, Price GD.** 2002. Evolution and diversity of CO_2 concentrating mechanisms in cyanobacteria. Functional Plant Biology 29:161–173.
71. **Badger MR, Price GD.** 2003. CO_2 concentrating mechanisms in cyanobacteria: molecular components, their diversity and evolution. J Exp Bot 54:609–622.
72. **Cannon GC, Heinhorst S, Bradburne CE, Shively JM.** 2002. Carboxysome genomics: a status report. Functional Plant Biology 29:175–182.
73. **Holthuijzen YA, Vanbreemen JFL, Konings WN, Vanbruggen EFJ.** 1986. Electron microscopic studies of carboxysomes of *Thiobacillus neapolitanus*. Arch Microbiol 144:258–262.
74. **Peters KR.** 1974. [Characterization of a phage-like particle from cells of Nitrobacter. II. Structure and size (author's transl)]. Arch Microbiol. 97:129–140.
75. **Lancu CV, Ding HJ, Morris DM, Dias DP, Gonzales AD,** et al. 2007. The structure of isolated Synechococcus strain WH8102 carboxysomes as revealed by electron cryotomography. J Mol Biol 372:764–773.
76. **Schmid MF, Paredes AM, Khant HA, Soyer F, Aldrich HC**, et al. 2006. Structure of *Halothiobacillus neapolitanus* carboxysomes by cryoelectron tomography. J Mol Biol 364:526–535.
77. **Kaneko Y, Danev R, Nagayama K, Nakamoto H.** 2006. Intact carboxysomes in a cyanobacterial cell visualized by hilbert differential contrast transmission electron microscopy. J Bacteriol 188:805–818.

78. **Tsai Y, Sawaya MR, Cannon GC, Cai F, Williams EB,** et al. 2007. Structural analysis of CsoS1A and the protein shell of the *Halothiobacillus neapolitanus* carboxysome. PLoS Biol 5:e144.
79. **Tanaka S, Yeates TO.** unpublished results.
80. **Celeste L. V. Johnson, Marian L. Buszko, and Thomas A. Bobik.** 2004. Purification and Initial Characterization of the Salmonella enterica PduO ATP:Cob(I)alamin Adenosyltransferase. J Bacteriol 186: 7881-7887.81.
81. **Tobimatsu T,Kawata M,Toraya T.** 2005. The N-terminal regions of beta and gamma subunits lower the solubility of adenosylcobalamin-dependent diol dehydratase. Biosci Biotechnol Biochem 69:455–462.
82. **Price GD, Howitt SM, Harrison K, Badger MR.** 1993. Analysis of a genomic DNA region from the cyanobacterium *Synechococcus* sp. strain PCC7942 involved in carboxysome assembly and function. J.Bacteriol.175:2871–79.
83. **Harlow, E., and D. Lane.** 1988. Antibodies: a laboratory manual. Cold Spring Harbor Laboratory, Cold Spring Harbor, N.Y.
84. **Bobik TA.** unpublished data 2008.
85. **Shouqiang Cheng, Yu Liu, Christopher S. Crowley, Todd O.Yeates, and Thomas A. Bobik.** 2008. Bacterial microcompartments: their properties and paradoxes. BioEssays 30:1084–1095.
86. **Sampson EM, Bobik TA.** 2008. Microcompartments for B_{12}-dependent 1,2-propanediol degradation provide protection from DNA and cellular damage by a reactive metabolic intermediate. J Bacteriol 190:2966–2971.
87. **Mori K, Tobimatsu T, Hara T, Toraya T.** 1997. Characterization, sequencing, and expression of the genes encoding a reactivating factor for glycerol-inactivated adenosylcobalamin-dependent diol dehydratase. J Biol Chem 272: 32034–32041.
88. **Mori K, Tobimatsu T, Toraya T.** 1997. A protein factor is essential for in situ reactivation of glycerol-inactivated adenosylcobalamin dependent diol dehydratase. Biosci Biotechnol Biochem 61:1729–1733.
89. **Mori K, Toraya T.** 1999. Mechanism of reactivation of coenzyme B12-dependent diol dehydratase by a molecular chaperone-like reactivating factor. Biochemistry 38:13170–13178.
90. **Rondon MR, Escalante-Semerena JC.** 1992. The poc locus is required for 1,2-propanediol-dependent transcription of the cobalamin biosynthetic (cob) and propanediol utilization (pdu) genes of Salmonella typhimurium. J Bacteriol 174:2267–2272.
91. **Rondon MR, Horswill RA, Escalante-Semerena KC.** 1995. DNA polymerase I function is required for the utilization of ethanolamine, 1,2-propanediol, and propionate by Salmonella typhimurium LT2. J Bacteriol. 177:7119–7124.
92. **Rondon MR, Kazmierczak R, Escalante-Semerena JC.** 1995. Glutathione is required for maximal transcription of the cobalamin biosynthetic and 1,2-propanediol utilization (cob/pdu) regulon and for the catabolism of ethanolamine, 1,2-propanediol, and propionate in Salmonella typhimurium. J Bacteriol 177:5434–5439.
93. Crowley CS, Sawaya MR, Bobik TA, Yeates TO. unpublished results 2008.

94. **Hacking AJ, Aguilar J, Lin ECC.** 1978. Evolution of propanediol utilization in Escherichia coli mutants with improved substrate scavenging power. J Bacteriol 136:522–530.
95. **Allen RH, Stabler SP, Savage DG, Lindenbaum J.** 1993. Metabolic abnormalities in cobalamin (vitamin B12) folate deficiency. FASEB J.7:1344–53.
96. **Drummond JT, Matthews RG.** 1993. Cobalamin-dependent and cobalamin independent methionine synthases in *Escherichia coli*: two solutions to the same chemical problem. Adv. Exp. Med. Biol. 338:687–92.
97. **Taylor RT, Weisbach H.** 1973. N^5- methyltetrahydrofolate-homocysteine methyltransferases. In The Enzymes, ed. D Boyer, pp. 121–165. New York: Academic.